2.7. In situ hybridization

Sections of liver from rats 30 min after reperfusion were used. The sections were soaked in xylene, ethanol and target retrieval solution (DAKO, Carpinteria, CA, USA). After treatment with proteinase K (DAKO), the sections were immersed in 0.3% hydrogen peroxide solution.

As an antisense-NGFI-B probe, 40-mer synthetic FITC-labeled oligonucleotides (5′-GAAGGCTAGAATGTTGTCTATCCAGTCACCAAAGCCGCGG-3′) were developed and used. The sections were heated for 5 min on the surface of a 95°C hotplate and then incubated overnight in a humidified chamber at 37°C.

After treatment with avidin solution (DAKO), biotin solution (DAKO), peroxidase-labeled anti-FITC antibody (DAKO) and streptavidin–horseradish peroxidase, the sections were incubated with a solution containing hydrogen peroxide, biotinyl tyramide and 3,3′diaminobenzidine. The sections were counter-stained with hematoxylin.

The immunohistochemical analysis for hepatocytes was also performed in the ordinal way using monoclonal anti-hepatocyte antibody (DAKO, product # M7158).

2.8. Western blotting

The liver specimen was homogenized in SDS sample buffer and sonicated on ice to shear genomic DNA. An equal amount of protein was separated through a 10% SDS-polyacrylamide gel and electro-blotted onto a polyvinylidine difluoride membrane (Immobilon, Millipore, Bedford, MA, USA). Blots were incubated overnight at 4°C with the primary antibody; anti-phospho-Ser-133-specific cyclic adenosine-3′:5′-monophosphate response element binding (pCREB) polyclonal antibody (NEB, Beverly, MA, USA), and subsequently with a horseradish peroxidase-conjugated anti-rabbit IgG antibody (NEB). They were visualized with an electrogenerated chemiluminescence (ECL) Western Blotting System (Amersham).

To confirm the amount of CREB protein, blots were stripped off antibodies by incubating in stripping buffer (2% SDS, 62.5 mM Tris–HCl, 100 mM beta-mercaptoethanol) at 55°C for 30 min, and then re-probed with anti-CREB antibody (NEB).

2.9. Gel shift assay

Gel shift assays were performed with nuclear extract prepared from primary cultured rat liver hepatocytes (Sangi Pharmaceuticals, Sapporo, Japan). The Klenow-labeled double-strand DNA probe (cgtcccaTGGCGTCAcatTGACGTCTcgcattccagg) containing two copies of the putative CREB binding site (indicated by capital letters) was designed from the 5′ flanking region of the NOR-1 gene [15]. Proteins were mixed with 10,000 cpm of the labeled probe in the reaction buffer (20 mM *N*-2 hydroxyethylpiperazine-*N*′-2 ethanesulfonic acid (HEPES), 40 mM potassium chloride, 6% glycerol, 0.2 mM ethylenediaminetetraacetic acid (EDTA), 100 ng/ml poly(dI-dC) and 1 mM dithiothreitol (DTT)). The reaction mixture was incubated for 20 min at room temperature and then electrophoresed through a 5% non-denaturing polyacrylamide gel. For competition analysis, a 20-fold molar excess of homologous oligonucleotide was used.

2.10. Gene expression in the human liver

To confirm the universality of the results, quantitative mRNA analysis of NGFI-B family genes was performed in human specimens in triplicate.

From April 1, 1996 to September 31, 1996, 20 patients underwent partial hepatectomy for hepatocellular carcinoma at the Tokyo University Hospital. The operation consisted of Pringle's maneuver only [16]. Pringle's maneuver was performed using Fogarty forceps for 15 min, followed by a 5-min release period, and this schedule was repeated until hepatectomy was accomplished. Specimens were available from five of these patients. The operative procedure has been described in detail elsewhere [17].

Two liver specimens were taken from each patient: one before ischemia and one after hepatectomy. First, the area to be resected was stained by injecting indigo carmine into the portal venous branch under ultrasound guidance [17], and part of this area was sampled as the specimen before ischemic damage. After hepatectomy, another specimen was taken from part of the liver adjacent to the resected area [18]. The tissue samples were frozen immediately and stored until use.

The protocol was approved by the ethics committee of our local authority. Informed consent was obtained from each patient.

2.11. Statistical analysis

The data are expressed as mean ± standard deviation (Table 1).

The AST level and mRNA level of each gene were compared with the corresponding levels obtained just after reperfusion (0 min) using an analysis of variance (ANOVA) with Bonferroni's correction.

The effects of cycloheximide on plasma AST and the mRNA level of each gene during the observation period were examined by a two-way repeated-measures ANOVA.

The difference in the level of gene expression between before and after ischemia-reperfusion injury in the human specimens was analyzed by the unpaired Student's *t*-test.

Differences were considered to be significant at $P < 0.0033$ or $P < 0.005$ in ANOVA and at $P < 0.05$ in the other analyses.

3. Results

3.1. Changes in AST levels

The average AST level gradually increased after reperfusion in both groups (Fig. 1). Two-way repeated-measures ANOVA revealed that the AST levels of the two groups differed significantly during the observation period ($P = 0.0066$).

3.2. Detection of NGFI-B, NOR-1 and Nurr1 mRNA

NGFI-B mRNA expression was observed by Southern blotting in the livers of the sham-operated rats in both the control and cycloheximide groups (Fig. 2A). However, this

Table 1
Patients' profile

No.	Age/sex	ICGR15[a] (%)	Operation time (min)	Ischemic time (min)	Blood loss (ml)
1	63/M	17	213	120	990
2	59/F	5	360	185	390
3	66/F	8	565	240	1270
4	64/M	24	388	85	1060
5	68/M	14	470	105	1820

[a] Indocyanine green retention rate at 15 min.

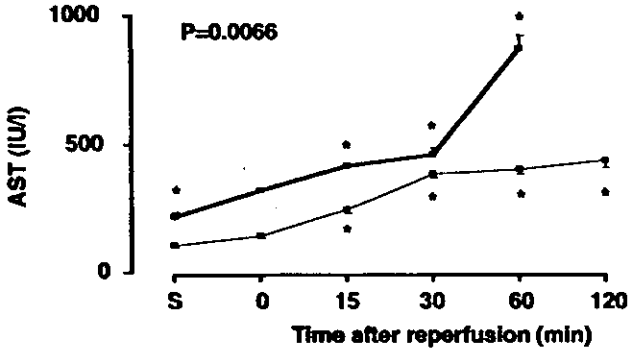

Fig. 1. Changes in plasma AST levels. Data are expressed as mean ± standard deviation. Thick line, cycloheximide group; thin line, control group ($n = 3$ for each group and each time). The effects of cycloheximide on the AST level (two-way repeated-measures ANOVA) are shown in the upper left corner. $^*P < 0.0033$ or $P < 0.005$ compared with the mean level at 0 min after reperfusion. S, sham operation.

expression level in the sham-operated rats was low. Quantitative mRNA analysis (Fig. 3A) revealed that NGFI-B mRNA expression in the rats in the control group reached a maximum 30 min after reperfusion. In the cycloheximide rats, this level continued to increase during the observation period. Two-way repeated-measures ANOVA revealed that the levels of NGFI-B mRNA expression in the two groups were not different during the observation period ($P = 0.11$).

For NOR-1, the mRNA expression level was maximum at 30 min after ischemic reperfusion, and then gradually decreased in the control group. In the cycloheximide

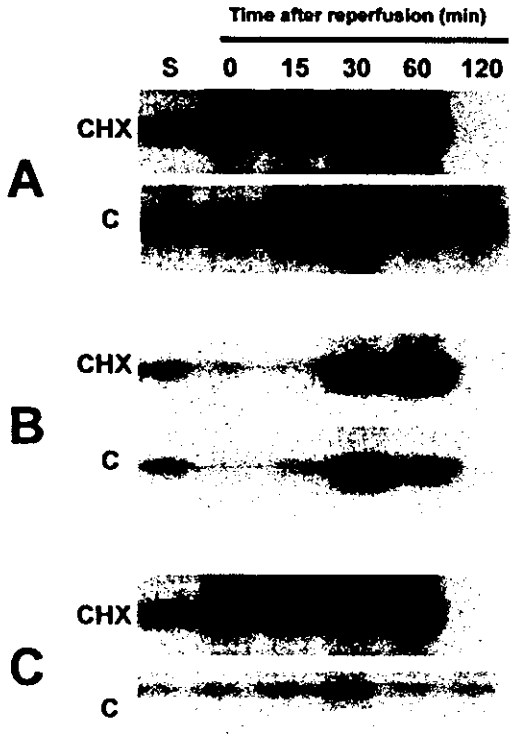

Fig. 2. NGFI-B (A), NOR-1 (B) and Nurr1 (C) gene expression in the rat. The left branches of both the portal vein and hepatic artery were clamped for 60 min. Sham surgery (S) was also performed. Part of the left lateral lobe was sampled at 0, 15, 30, 60 and 120 min after reperfusion in the presence (CHX) or absence (C) of cycloheximide. Total RNA (5 mg) was subjected to RT-PCR, transferred to a nylon membrane, hybridized and auto-radiographed.

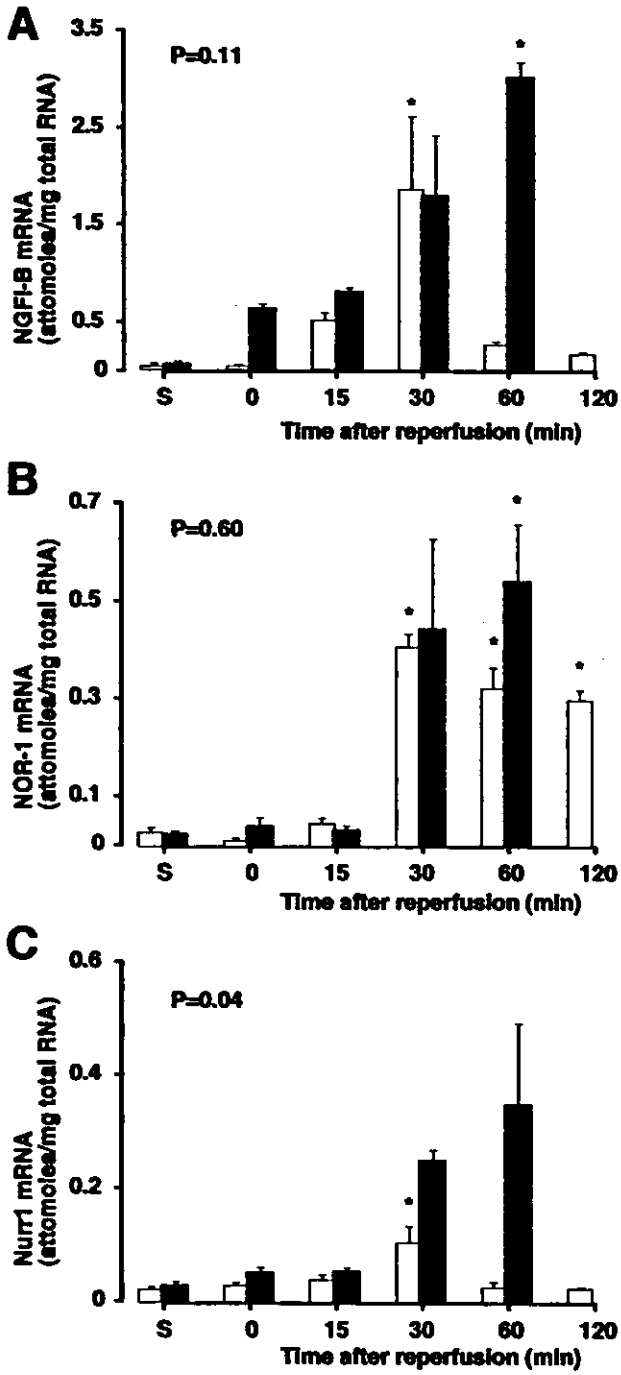

Fig. 3. Quantitative mRNA analysis of NGFI-B (A), NOR-1 (B) and Nurr1 (C) in rats. Black box, cycloheximide group; white box, control group ($n = 3$ for each group and each time). The effects of cycloheximide on the gene expression level (two-way repeated-measures ANOVA) are shown in the upper left corner. $^*P < 0.0033$ or $P < 0.005$ compared with the mean level at 0 min after reperfusion. S, sham operation.

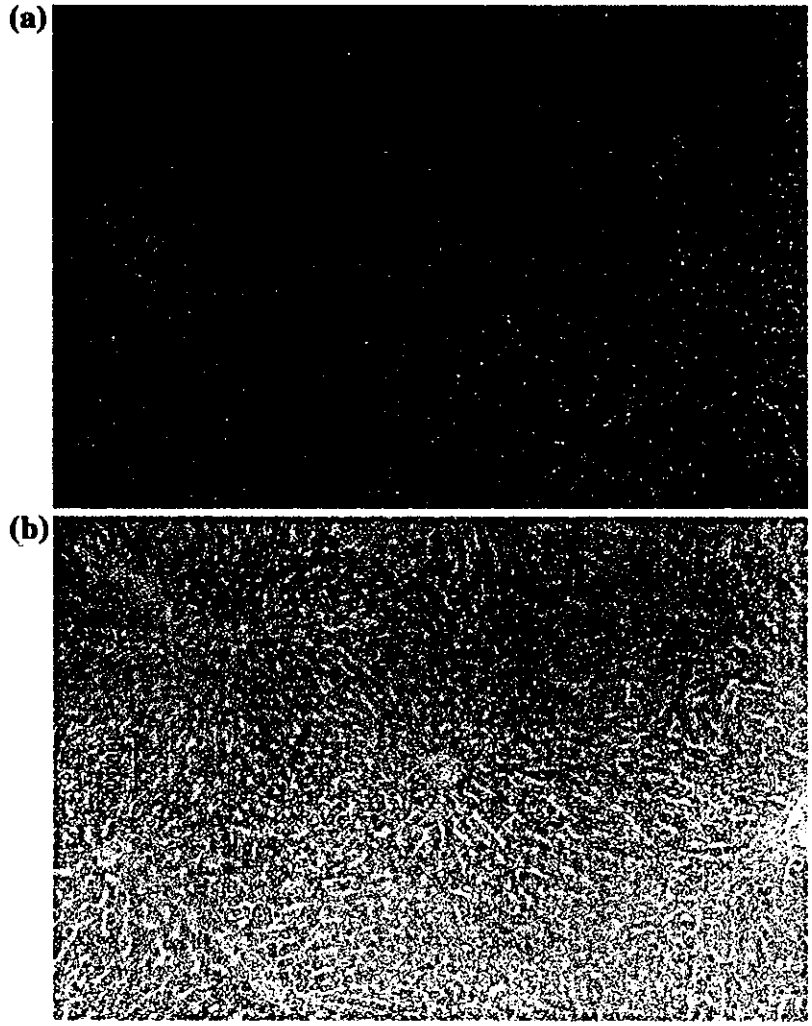

Fig. 4. Expression of NGFI-B mRNA (A) and immunohistochemical analysis of hepatocytes (B) in the liver from rats 30 min after reperfusion (original magnification, ×200). Note strong NGFI-B mRNA signals around the central vein.

group, the level continued to increase during the observation period.

A high expression of Nurr1 mRNA was detected at 30 min after reperfusion in the control group, and this rapidly decreased thereafter. In the cycloheximide group, the level continued to increase until 60 min after reperfusion.

3.3. In situ hybridization (Fig. 4)

NGFI-B mRNA was detected in specimens obtained 30 min after reperfusion. The strong signals were recognized in the hepatocytes around the central veins. In contrast, hepatocytes staining were uniform in degree.

3.4. Phosphorylation of CREB

In the cycloheximide rats, maximum phosphorylation of CREB at Ser 133 was detected at 30 min after reperfusion (Fig. 5). This phosphorylation persisted for 60 min.

In contrast, this phosphorylation was not detected in the liver in the control group. All of the samples showed equal amounts of CREB protein as determined using anti-CREB antibody.

3.5. Gel shift assay (Fig. 6)

Hepatocyte nuclear extracts produced a protein–nucleotide complex that migrated to two different positions (lane

Fig. 5. Detection of pCREB (upper panel) and CREB (lower panel) protein in rat specimens from the cycloheximide group. PC12 cells that had been incubated with 10 mM forskolin for 30 min were used as a positive control.

Fig. 6. Gel shift assay. Hepatocyte nuclear extracts produced a protein–nucleotide complex that migrated to two different positions (lane 1). A 20-fold molar excess of the competitor efficiently eliminated both complexes (lane 2). The locations of shifted bands are indicated with arrows.

1). A 20-fold molar excess of the competitor efficiently eliminated both complexes (lane 2).

3.6. Quantitative gene analysis in human specimens

NGFI-B mRNA expression was observed by Southern blotting in all of the human specimens analyzed (Fig. 7A). Quantitative mRNA analysis (Fig. 8A) revealed that NGFI-B mRNA expression in specimens after reperfusion was stronger than that before ischemic insult in four of five cases.

Similar results were obtained for NOR-1 and Nurr1 mRNA.

4. Discussion

We examined the gene expression of NGFI-B, NOR-1 and Nurr1 as potential determinants of tissue ischemia-reperfusion injury in rats and humans. NGFI-B mRNA was detected in hepatocytes around the central veins. Since it has been reported that hepatocytes in the central lobes suffer most readily from warm ischemic injury [19], NGFI-B mRNA may have been induced by ischemic injury. Our experiments

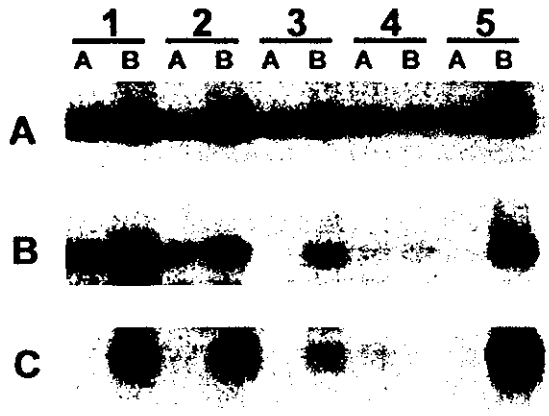

Fig. 7. NGFI-B (A), NOR-1 (B) and Nurr1 (C) gene expression in human liver. Two liver specimens were taken from each patient: one before ischemia (A) and one after hepatectomy (B). Total RNA (5 mg) was subjected to RT-PCR, transferred to a nylon membrane, hybridized and auto-radiographed. The number shown is that of the patient.

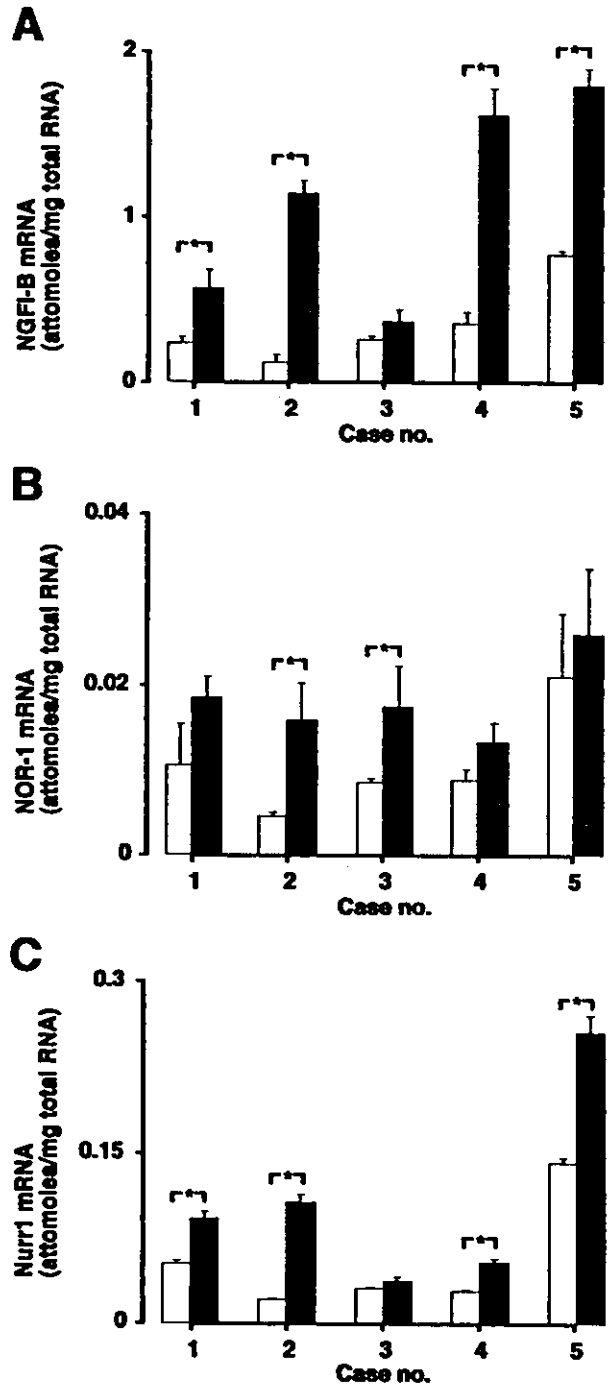

Fig. 8. Quantitative mRNA analysis of NGFI-B (A), NOR-1 (B) and Nurr1 (C) in human liver. Black, after hepatectomy; white, before ischemia. The measurement was performed in triplicate. *$P < 0.05$ compared with the expression level of two liver specimens from the same patient.

revealed that these genes were rapidly and transiently induced after reperfusion. The expression patterns were typical of immediate-early genes, as is often seen in other biological systems involving c-fos, c-jun and junB [20,21].

NGFI-B, NOR-1 and Nurr1 are highly homologous with regard to their amino acid sequences, but show some differences in gene expression patterns [14,22], dimer formation [7] and transcriptional activity [23]. In our study, these family members showed different levels of expression; the expression level of NBFI-B was approximately 100 times that of NOR-1 and 10 times that of Nurr1 in human livers. These differences among the NGFI-B family genes suggest distinct functional roles in the liver following ischemia-reperfusion injury.

The phosphorylation of CREB was strongly detected as early as 15 min after reperfusion, while the amount of CREB remained constant. We previously suggested that the pathway via CREB and CRE is responsible for the early induction of NOR-1 in a human breast cancer cell line, MCF-7, during cell death induced by A23187 stimulation [24]. The expression of genes containing CREs is mediated by the binding of CREB to CREs [25]. In addition, the transcriptional activity of CREB is regulated by phosphorylation at Ser 133 [26]. CREB binding sites have been found in the promoter region in the NGFI-B gene family [4–6]. CREB bound to the promoter region of the NOR-1 gene was suggested by the present assay. Although the role of immediate-early genes in ischemia-reperfusion injury remains unclear, these findings suggest that the pathway via CREB and CRE is responsible for the early induction of NGFI-B family genes during liver ischemia-reperfusion injury in the rat [27].

In conclusion, we recognized the early induction of NGFI-B family genes after ischemia-reperfusion injury in rat and human livers. The pathway via CREB and CRE may be responsible for the early induction of these genes.

Acknowledgements

This work is supported in part by a Grand-in-aid for Scientific Research from the Ministry of Education, Science and Culture of Japan and a Grant-in-aid for Research on Human genome, Tissue engineering, Food biotechnology, Health sciences research grants, Ministry of Health, Labor and Welfare of Japan.

References

[1] Evans RM. The steroid and thyroid hormone receptor superfamily. Science 1988;240:889–895.
[2] Mangelsdorf DJ, Thummel C, Beato M, Herrlich P, Schutz G, Umesono K, et al. The nuclear receptor superfamily: the second decade. Cell 1995;83:835–839.
[3] Maruyama K, Tsukada T, Ohkura N, Bandoh S, Hosono T, Yamaguchi K. The NGFI-B subfamily of the nuclear receptor superfamily. Int J Oncol 1998;12:1237–1243.
[4] Milbrandt J. Nerve growth factor induces a gene homologous to the glucocorticoid receptor gene. Neuron 1988;1:183–188.
[5] Law SW, Conneely OM, DeMayo FJ, O'Malley BW. Identification of a new brain-specific transcription factor, NURR1. Mol Endocrinol 1992;6:2129–2135.
[6] Ohkura N, Hijikuro M, Yamamoto A, Miki K. Molecular cloning of a novel thyroid/steroid receptor superfamily gene from cultured rat neuronal cells. Biochem Biophys Res Commun 1994;205:1959–1965.
[7] Zetterstrom RH, Solomin L, Mitsiadis T, Olson L, Perlmann T. Retinoid X receptor heterodimerization and developmental expression distinguish the orphan nuclear receptors NGFI-B, Nurr1, and Nor1. Mol Endocrinol 1996;10:1656–1666.
[8] Maruyama K, Tsukada T, Bandoh S, Sasaki K, Ohkura N, Yamaguchi K. Expression of NOR-1 and its closely related members of the steroid/thyroid hormone receptor superfamily in human neuroblastoma cell lines. Cancer Lett 1995;96:117–122.
[9] Ohkura N, Hijikuro M, Miki K. Antisense oligonucleotide to NOR-1, a novel orphan nuclear receptor, induces migration and neurite extension of cultured forebrain cells. Brain Res Mol Brain Res 1996;35:309–313.
[10] Zetterstrom RH, Solomin L, Jansson L, Hoffer BJ, Olson L, Perlmann T. Dopamine neuron agenesis in Nurr1-deficient mice. Science 1997;276:248–250.
[11] Scearce LM, Laz TM, Hazel TG, Lau LF, Taub R. RNR-1, a nuclear receptor in the NGFI-B/Nur77 family that is rapidly induced in regenerating liver. J Biol Chem 1993;268:8855–8861.
[12] Trautwein C, Rakemann T, Pietrangelo A, Plumpe J, Montosi G, Manns MP. C/EBP-beta/LAP controls down-regulation of albumin gene transcription during liver regeneration. J Biol Chem 1996;271:22262–22270.
[13] Chomczynski P, Sacchi N. Single-step method of RNA isolation by acid guanidinium thiocyanate-phenol-chloroform extraction. Anal Biochem 1987;162:156–159.
[14] Bandoh S, Tsukada T, Maruyama K, Ohkura N, Yamaguchi K. Differential expression of NGFI-B and RNR-1 genes in various tissues and developing brain of the rat: comparative study by quantitative reverse transcription-polymerase chain reaction. J Neuroendocrinol 1997;9:3–8.
[15] Ohkura N, Ito M, Tsukada T, Sasaki K, Yamaguchi K, Miki K. Alternative splicing generates isoforms of human neuron-derived orphan receptor-1 (NOR-1) mRNA. Gene 1998;211:79–85.
[16] Pringle JH. Notes on the arrest of hepatic hemorrhage due to trauma. Ann Surg 1908;48:541–549.
[17] Makuuchi M, Hasegawa H, Yamazaki S. Ultrasonically guided subsegmentectomy. Surg Gynecol Obstet 1985;161:346–350.
[18] Sugawara Y, Kubota K, Ogura T, Esumi H, Inoue K, Takayama T, et al. Increased nitric oxide production in the liver in the perioperative period of partial hepatectomy with Pringle's maneuver. J Hepatol 1998;28:212–220.
[19] Harvey PRC, Iu S, McKeown CMB, Petrunka CN, Ilson RG, Strasberg SM. Adenine nucleotide tissue concentrations and liver allograft viability after cold preservation and warm ischemia. Transplantation 1988;45:1016–1020.
[20] Sassone-Corsi P, Visvader J, Ferland L, Mellon PL, Verma IM. Induction of proto-oncogene fos transcription through the adenylate cyclase pathway: characterization of a cAMP-responsive element. Genes Dev 1988;2:1529–1538.
[21] Ginty DD, Fanger GR, Wagner JA, Maue RA. The activity of cAMP-dependent protein kinase is required at a posttranslational level for induction of voltage-dependent sodium channels by peptide growth factors in PC12 cells. J Cell Biol 1992;116:1465–1473.
[22] Maruyama K, Tsukada T, Bandoh S, Sasaki K, Ohkura N, Yamaguchi K. Expression of the putative transcription factor NOR-1 in the nervous, the endocrine and the immune systems and the developing brain of the rat. Neuroendocrinology 1997;65:2–8.
[23] Maruyama K, Tsukada T, Bandoh S, Sasaki K, Ohkura N, Yamaguchi

K. Retinoic acids differentially regulate NOR-1 and its closely related orphan nuclear receptor genes in breast cancer cell line MCF-7. Biochem Biophys Res Commun 1997;231:417–420.

[24] Ohkubo T, Ohkura N, Maruyama K, Sasaki K, Nagasaki K, Hanzawa H, et al. Early induction of the orphan nuclear receptor NOR-1 during cell death of the human breast cancer cell line MCF-7. Mol Cell Endocrinol 2000;162:151–156.

[25] Montminy MR, Bilezikjian LM. Binding of a nuclear protein to the cyclic-AMP response element of the somatostatin gene. Nature 1987;328:175–178.

[26] Gonzalez GA, Montminy MR. Cyclic AMP stimulates somatostatin gene transcription by phosphorylation of CREB at serine 133. Cell 1989;59:675–680.

[27] Ledda-Columbano GM, Coni P, Faa G, Manenti G, Columbano A. Rapid induction of apoptosis in rat liver by cycloheximide. Am J Pathol 1992;140:545–549.

THE JOURNAL OF BIOLOGICAL CHEMISTRY
Vol. 278, No. 40, Issue of October 3, pp. 38796–38802, 2003
Printed in U.S.A.

A Novel Mitochondrial Carnitine-acylcarnitine Translocase Induced by Partial Hepatectomy and Fasting*

Received for publication, June 16, 2003, and in revised form, July 24, 2003
Published, JBC Papers in Press, July 25, 2003, DOI 10.1074/jbc.M306372200

Ei Sekoguchi‡§¶, Norihiro Sato‖, Akihiro Yasui§, Shinji Fukada§, Yuji Nimura¶, Hiroyuki Aburatani, Kyoji Ikeda‡, and Akira Matsuura‡ ‡‡**

*From the ‡Department of Geriatric Research, National Institute for Longevity Sciences, Obu, Aichi 474-8522, Japan, the §Chubu National Hospital, Obu, Aichi 474-8522, Japan, the ¶Nagoya University Graduate School of Medicine, Showa-ku, Nagoya 466-8550, Japan, the ‖Tokyo University of Pharmacy and Life Science, Hachioji 192-0392, Japan, and the **Research Center for Advanced Science and Technology, University of Tokyo, Meguro-ku, Tokyo 153-8904, Japan*

The carnitine-dependent transport of long-chain fatty acids is essential for fatty acid catabolism. In this system, the fatty acid moiety of acyl-CoA is transferred enzymatically to carnitine, and the resultant product, acylcarnitine, is imported into the mitochondrial matrix through a transporter named carnitine-acylcarnitine translocase (CACT). Here we report a novel mammalian protein homologous to CACT. The protein, designated as CACL (CACT-like), is localized to the mitochondria and has palmitoylcarnitine transporting activity. The tissue distribution of CACL is similar to that of CACT; both are expressed at a higher level in tissues using fatty acids as fuels, except in the brain, where only CACL is expressed. In addition, CACL is induced by partial hepatectomy or fasting. Thus, CACL may play an important role cooperatively with its homologue CACT in a stress-induced change of lipid metabolism, and may be specialized for the metabolism of a distinct class of fatty acids involved in brain function.

Long-chain polyunsaturated fatty acids, such as arachidonic acid and docosahexaenoic acid, are important nutritional components, serving as structural elements in mammalian cells. They confer fluidity, flexibility, and selective permeability to cellular membranes, and affect cellular and physiological processes (1). In addition, long-chain fatty acids are used as an energy source through the mitochondrial β-oxidation pathway, especially in tissues such as muscle, during periods of fasting and other metabolic stress (2).

The carnitine shuttle system in eukaryotic cells provides for the entry of long-chain fatty acids into the mitochondrial matrix, where β-oxidation takes place (3, 4). Acyl-CoA pools supply activated substrates for many key metabolic pathways, such as the tricarboxylic acid cycle and lipid synthesis. A wide range of activated acyl groups is transferred reversibly from acyl-CoA to carnitine through the actions of carnitine acyltransferases. The transfer from the limited pools of membrane-impermeable CoA to the abundant and mobile carnitine allows transport between compartments.

Acylcarnitines are imported into mitochondria through carnitine-acylcarnitine translocase (CACT)[1] (5, 6). This protein catalyzes a mole to mole exchange of carnitines and acylcarnitines, thereby permitting the fatty acid moieties to be translocated into the mitochondrial matrix. Several cases of CACT deficiency have been reported (7–9). Patients with these defects generally present in early infancy with acute, potentially life-threatening episodes of hypoketotic hypoglycemic coma, induced by fasting during intercurrent disease. The clinical features of these patients include hypoketotic hypoglycemia, mild hyperammonemia, variable dicarboxylic aciduria, hepatomegaly with abnormal liver functions, various cardiac symptoms, and skeletal muscle weakness.

In a search for genes that are up-regulated during liver regeneration after partial hepatectomy in rodents, we found a novel gene that encodes a protein homologous to CACT. Here we report the characterization of the gene product, CACL (for carnitine-acylcarnitine translocase-like). The protein exhibits a mitochondrial carnitine-acylcarnitine translocase activity, and its expression is induced by stresses such as hepatectomy and fasting.

EXPERIMENTAL PROCEDURES

Animals—Eight-week-old C57BL/6J male mice were purchased from CLEA Japan Inc. (Tokyo, Japan). Animals were kept in a temperature-controlled animal room with a 12-h dark/light cycle and were maintained on a commercially available diet (CE-2, CLEA Japan Inc.) consisting (by energy) of 29.2% protein, 58.8% carbohydrates, and 12.0% fat. Mice were either fed *ad libitum* or fasted for 48 h, and had free access to water. A 70% partial hepatectomy was performed according to the method of Higgins and Anderson (10). The surgery was performed between 8 and 11 a.m. under ether anesthesia. Animals were sacrificed before partial hepatectomy and at 6, 12, 24, and 48 h after the operation. Hearts, livers, brains, and kidneys were excised, immediately frozen in liquid nitrogen, and stored at −80 °C. All experiments were conducted in accordance with the animal care guidelines of the National Institute for Longevity Sciences (Obu, Japan).

Cell Lines and Culture Conditions—NIH3T3 murine fibroblasts were maintained as monolayer cultures in Dulbecco's modified minimal essential medium (Sigma) supplemented with 10% (v/v) fetal bovine serum (ICN Biomedicals Inc., Aurora, OH), penicillin (100 units/ml), and streptomycin (100 μg/ml; Invitrogen Corp.) at 37 °C in a humidified atmosphere containing 95% air and 5% CO_2. The GP2-293 retroviral packaging cell line was obtained from Clontech (Palo Alto, CA) and was maintained as monolayer cultures in Dulbecco's modified essential medium supplemented with 10% heat-inactivated fetal bovine serum. Puromycin (Sigma) was added at a final concentration of 3 μg/ml for the selection of pMXpuro-infected cells.

Construction of Plasmids—A retroviral vector derived from a murine leukemia virus, pMXpuro (11), was kindly provided by Prof. T. Kitamura (University of Tokyo, Tokyo, Japan). Open reading frame regions

* This work was supported in part by a grant from the Ministry of Health, Labor, and Welfare (to A. M.). The costs of publication of this article were defrayed in part by the payment of page charges. This article must therefore be hereby marked "*advertisement*" in accordance with 18 U.S.C. Section 1734 solely to indicate this fact.

‡‡ To whom correspondence should be addressed. Tel./Fax: 81-562-44-6595; E-mail: amatsuur@nils.go.jp.

[1] The abbreviations used are: CACT, carnitine-acylcarnitine translocase; CACL, carnitine-acylcarnitine translocase-like; PBS, phosphate-buffered saline; PH, partial hepatectomy; MOPS, 3-morpholinopropanesulfonic acid.

of *mCACT* and *mCACL* were amplified by PCR using EST clones ME624844 and BE372112 as templates, respectively, and cloned into the *Bam*HI-*Bst*XI sites of pMXpuro. For epitope tagging of CACL, a myc-His_6 tag of the pEF4/mycHis vector (Invitrogen Corp.) was inserted immediately before the termination codon of *mCACL* cDNA, and the fusion gene was cloned into the pMXpuro vector.

For the functional expression of *mCACL* in yeast cells, the 1.2-kb *Eco*RI-*Eco*RV fragment of *mCACL* cDNA was inserted into the *Eco*RI-*Puu*II sites of pKT10 (12). The resultant plasmid, pKT10-mCACL, expressed mCACL driven by promoter of *TDH3*, a gene for glyceraldehyde-3-phosphate dehydrogenase of the budding yeast. The p316CRC1 plasmid was constructed by inserting the yeast gene for CACT (*CRC1*) into the pRS316 vector (13).

For the expression of *mCACL* in *Escherichia coli* cells, the 0.9-kb *Bam*HI-*Xho*I fragment of *mCACL* was isolated from the pMXpuro/mCACL plasmid and inserted into the *Bgl*II-*Sal*I sites of pBAD/gIIIA (Invitrogen Corp.). The resultant plasmid pBAD/CACL-His_6 encoded a CACL-His_6 fusion protein with the pIII signal sequence at the amino terminus, which allowed the recombinant protein to be secreted to plasma membranes. Expression of the fusion protein was induced by the addition of 0.2% arabinose to the LB medium.

Northern Blotting—Total RNA was isolated with TRIzol reagent (Invitrogen Corp.) according to the manufacturer's instructions. Poly(A)$^+$ RNA was isolated from total RNA with a Micro-FastTrack mRNA isolation kit (Invitrogen Corp.) and used for Northern blotting. Poly(A)$^+$ RNA (5 μg) was size-fractionated on a denaturing gel (1.2% agarose, 3.4% formaldehyde, 1× MOPS), transferred to a nylon membrane (Hybond-N, Amersham Biosciences) by capillary transfer, and fixed using standard techniques. A mouse multiple tissue Northern blot (number 7762-1) was purchased from Clontech. After prehybridization, the filters were probed with a 200-bp *CACL* or a 905-bp *CACT* cDNA fragment. An 857-bp β-actin fragment and a 400-bp β_2-microglobulin fragment of mouse were used as controls. The cDNA probes were labeled with [α-^{32}P]dCTP (3000 Ci/mmol; Amersham Biosciences) to a specific activity of >0.5 cpm/μg of DNA using the Megaprime DNA labeling system (Amersham Biosciences).

Antibodies—The following antibodies were purchased: anti-His_6 polyclonal antibody (Medical & Biological Laboratories Co. Ltd., Nagoya, Japan), anti-myc monoclonal antibody (clone 9E10, CRP Inc., Denver, PA), anti-p53 monoclonal antibody (Ab-6, EMD Biosciences, Inc., Darmstadt, Germany), and anti-β-actin monoclonal antibody (clone AC-15, Sigma). Sheep polyclonal antibodies against CACT (14) were gifts from Dr. V. A. Zammit (Hannah Research Institute, Ayr, Scotland, United Kingdom). Anti-mouse CACL polyclonal antibodies were produced as follows. A cDNA fragment corresponding to the carboxyl-terminal 31 amino acids of mouse CACL was inserted into the pGEX-4T-2 vector (Amersham Biosciences). Glutathione *S*-transferase-mCACL fusion protein was produced in *E. coli* DH5α cells and was used as an antigen for immunizing rabbits. The antibodies were affinity purified against an MBP-mCACL fusion protein produced in *E. coli*.

Western Blot Analysis—NIH3T3 cells were washed twice with PBS and suspended in a lysis buffer containing 20 mM Tris-HCl, pH 7.4, 150 mM NaCl, 2 mM EDTA, 1% Nonidet P-40, 1% Na deoxycholate, 0.1% SDS, 50 mM NaF, 1 mM dithiothreitol, 1 mM phenylmethylsulfonyl fluoride, and 1 mM Na_3VO_4. Frozen tissues were disrupted with a Multi-Beads Shocker (Yasui Kikai Co., Osaka, Japan) in 10 volumes of a buffer containing 0.25 M sucrose and 20 mM HEPES, and the homogenate was centrifuged at 600 × *g* for 10 min. The supernatant containing the postnuclear fraction was used as the protein lysate.

The protein lysates were incubated in 2× loading buffer (100 mM Tris-HCl, pH 6.8, 4% SDS, 20% glycerol, and 12% β-mercaptoethanol) at 42 °C for 30 min, separated by SDS-PAGE in a 10% gel, and electroblotted onto polyvinylidene difluoride membranes. To verify the equal loading of proteins in each lane, the blotted membrane was stained with Ponceau-S solution (Sigma). The membranes were blocked in 5% nonfat dry milk in PBS containing 0.1% Tween 20. Immunoblotting was performed with the primary antibodies at dilutions of 1:100 for anti-mCACL, and 1:1000 for anti-CACT and anti-His_6. The incubation with rabbit anti-mCACL antibodies was performed at 4 °C overnight, whereas the incubation with the other antibodies was at room temperature for 1 h. After washing, the membranes were incubated for 60 min with a horseradish peroxidase-conjugated secondary antibody diluted in PBS containing 0.5% nonfat dry milk and 0.1% Tween 20. Blots were developed by enhanced chemiluminescence according to the manufacturer's instructions (ECL Western blotting detection system, Amersham Biosciences).

Immunocytochemistry—Cells were fixed in 4% paraformaldehyde/PBS at room temperature for 10 min and permeabilized with 0.1% Triton X-100 in PBS for 10 min. Cells were then washed in PBS and incubated for 30 min with a blocking solution of 2% normal goat serum in PBS. Coverslips were then incubated for 1 h with the anti-CACL primary antibody diluted at 1:100 in PBS. After three 15-min washes in PBS, cells were incubated with secondary biotinylated anti-rabbit IgG antibody labeled with green fluorescent Alexa Fluor 488 (Molecular Probes Inc., Eugene, OR) at a 1:500 dilution in PBS for 1 h. Cells were washed again with PBS and mounted on glass slides with Vectashield (Vector Laboratories Inc., Burlingame, CA). To stain the mitochondria, 200 nM of a mitochondrion-specific dye (Mitotracker; Molecular Probes Inc.) was incubated with the cells for 30 min before fixation. Slides were examined on a confocal microscope (BX-FLA, Olympus, Tokyo, Japan) equipped for epifluorescence. Montages of images were prepared using PhotoShop 5.0 (Adobe Systems Inc., San Jose, CA).

Complementation of Yeast Mutation—Saccharomyces cerevisiae mutants defective in *CIT2* (for peroxisomal citrate synthase) or *CRC1* (for mitochondrial CACT) were obtained from Open Biosystems (Huntsville, AL). A *Δcit2::kanMX Δcrc1::kanMX* double mutant was constructed by a standard genetic cross. Yeast transformants were selected and grown on minimal medium containing 0.67% yeast nitrogen base without amino acids (YNB-WO, BD Diagnostic Systems, Sparks, MD) supplemented with 0.3% glucose and the appropriate amino acids. Minimal oleate medium contained YNB-WO with amino acids and 0.12% oleate, 0.2% Tween 40 as described previously (15).

Mitochondrial Preparations and Transport Assay—The transport of palmitoyl-[^{14}C]carnitine into mitochondria was measured as described previously (16). Cells grown to confluence on four dishes (15 cm in diameter) were washed twice with PBS and collected by centrifugation at 300 × *g* for 5 min. The cells were resuspended in 2 ml of a homogenization buffer containing 0.25 mM sucrose and 20 mM HEPES, pH 7.5, and were homogenized with 20 strokes in a Potter-Elvehjem (Teflon glass) homogenizer. The homogenate was centrifuged at 1,000 × *g* for 7 min. The resultant pellet was homogenized with 2 ml of the buffer and centrifuged again. The postnuclear supernatant was centrifuged at 2,000 × *g* for 30 min to obtain the mitochondrial fraction. The pellet, which contained ~0.2 mg of mitochondria, was resuspended in 250 μl of assay mixture containing 250 mM mannitol, 25 mM HEPES, pH 7.4, 50 μM EDTA, 3 mM ADP, 1 mM maleic acid, 5 mM potassium phosphate, pH 7.4, and palmitoyl-[^{14}C]carnitine (NEC-667, PerkinElmer Life Sciences)-bovine serum albumin complex (at a ratio of 1:3). Protein concentrations were determined using the BCA protein assay kit (Pierce).

Reconstitution of Carnitine-acylcarnitine Translocase in E. coli Cells—The plasmid pBAD/CACL-His_6 or the control vector pBAD/gIIIA was introduced into the *E. coli* strain Rosetta (F^- *ompT* $hsdS_B$ (r_B^- m_B^-) *gal dcm lacY1* pRARE(Cm^R); EMD Biosciences, Inc.). The transformants were grown in LB medium containing 0.2% L-arabinose for 18 h at 30 °C. The cultures were diluted with LB, and the transport reaction was initiated by the addition of palmitoyl-[^{14}C]carnitine (NEC-667, PerkinElmer Life Sciences) to the final concentration of 35 μM. After the reaction at 30 °C, cells were washed twice with PBS, and the incorporation of ^{14}C into the cells was quantified using an LSC-5100 liquid scintillation counter (Aloka, Tokyo, Japan).

Statistical Analysis—Data are expressed as mean ± S.D. The statistical significance of the differences between the control and the experimental group was determined by the unpaired Student's *t* test. Differences were considered significant at $p < 0.05$.

RESULTS

Identification of a Novel Protein Homologous to Carnitine-acylcarnitine Translocase—During a microarray analysis for genes induced after 70% partial hepatectomy (PH) in rats, we found a novel gene whose expression peaked at 6 h after the surgery (data not shown). A mouse clone homologous to the rat gene was obtained from the I.M.A.G.E. consortium, and the sequence analysis of the full-length cDNA identified an open reading frame of 918 nucleotides (Fig. 1*A*). The deduced protein, possessing six membrane-spanning regions (Fig. 1*B*), displayed homology with mitochondrial carrier family proteins. The protein showed the highest similarity (37% identity) with CACT, an inner mitochondrial membrane protein that is essential for the import of long-chain fatty acid moieties into the mitochondrial matrix (6). Thus, we designated the protein as CACL. A data base search using the BLAST program revealed that it is a conserved protein whose homologues are present in human, fly, and worm (Fig. 1*A*). The human orthologue

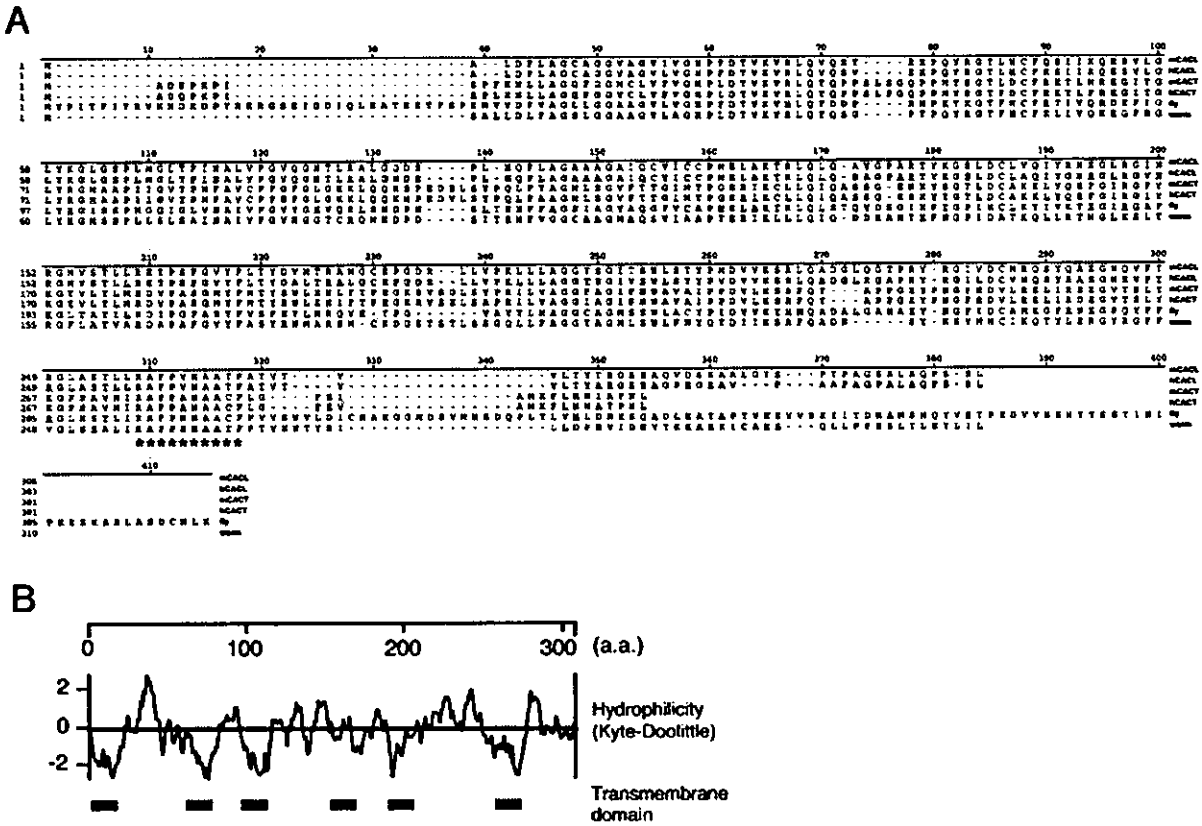

FIG. 1. **A novel CACL in mouse and human.** *A*, sequence alignment of CACLs with CACT. The deduced amino acid sequence of mouse CACL (*mCACL*) shows 37% identity with mouse and human CACT. The human homologue (*hCACL*) is highly conserved (97% identity to mCACL). A data base search identified homologues in *Caenorhabditis elegans* and *Drosophila melanogaster* (C54G10.4 and CG4995, respectively). Amino acid stretches characteristic of carnitine carriers (17) are marked with *asterisks*. *B*, hydrophilicity plot. Hydropathy scores were calculated by the method of Kyte and Doolittle (34). Putative transmembrane regions are shown with *lines*.

(hCACL) has 97% identity with mCACL at the amino acid level and is mapped on chromosome 14q32. A motif within the sixth hydrophobic domain, R(AS)(VF)PANAA(TC)F, has been shown to be conserved within the carnitine carrier subfamily (17). CACL and its homologous proteins all possess the motif, suggesting that they are involved in the transport of acylcarnitine across membranes.

Expression of CACL in Mouse Tissues—The expression pattern in tissues was surveyed using a mouse multiple tissue Northern blot filter. Mouse *CACL* mRNA, ~1.9 kb in length, was expressed in several tissues including heart, brain, liver, and kidney (Fig. 2). This pattern of expression was similar to that of its paralogue *mCACT*, except *CACT* mRNA was rare in brain tissue (Fig. 2*A*). The expression pattern was further confirmed by Western blot analysis using specific antibodies against CACL and CACT. The CACL protein was present at a comparable level in brain, liver, and kidney, whereas CACT expression was barely detectable in brain (Fig. 2*B*). These data suggest that CACL is involved in a biological process similar to that of CACT, but may play a specific role in certain tissues such as brain.

CACL Is Localized to Mitochondria—To determine the subcellular localization of the CACL protein, we constructed NIH3T3 mouse fibroblast cells that stably expressed a CACL fusion protein with a myc-His_6 tag in the carboxyl terminus. Using the anti-myc polyclonal antibody, CACL-myc-His_6 proteins in the fibroblasts were immunostained in a reticulated pattern, which coincided with the mitochondrial staining (Fig. 3, *A–C*). To exclude the possibility that the tag affected the subcellular localization of the protein, we further addressed the localization of CACL using an affinity purified antibody against mCACL. Although we could not detect specific signals of the endogenous protein (data not shown), overexpressed CACL protein without the tag was co-stained with the mitochondrial marker (Fig. 3, *D–F*). Based on these observations, we conclude that CACL, like its homologue CACT, is localized to mitochondria.

CACL Has Palmitoylcarnitine Transporting Activity—In yeast, the transport of acyl units to mitochondria is performed via two pathways, namely the glyoxylate cycle-mediated conversion of acetyl-CoA to succinate that occurs in peroxisomes and the carnitine-dependent acyl-CoA transport. The two pathways have been thought to act in parallel, because disruption of either the *CIT2* gene, which encodes the peroxisomal glyoxylate cycle enzyme citrate synthase, or one of the genes for the carnitine metabolism in mitochondria, did not affect the growth of yeast on oleate, whereas a mutant with both pathways disrupted failed to grow on the plate because of an inability to oxidize the fatty acid (18).

We constructed a double mutant defective in *CIT2* and *CRC1*, the mitochondrial CACT gene in yeast. As reported previously (15), the Δ*crc1* Δ*cit2* mutant could not form colonies on minimal medium containing oleate (Fig. 4*A*), and the defect was rescued by the introduction of the wild-type *CRC1* gene (Fig. 4*B*). Similarly, the heterologous expression of *mCACL* could relieve the growth impairment of the double mutant on

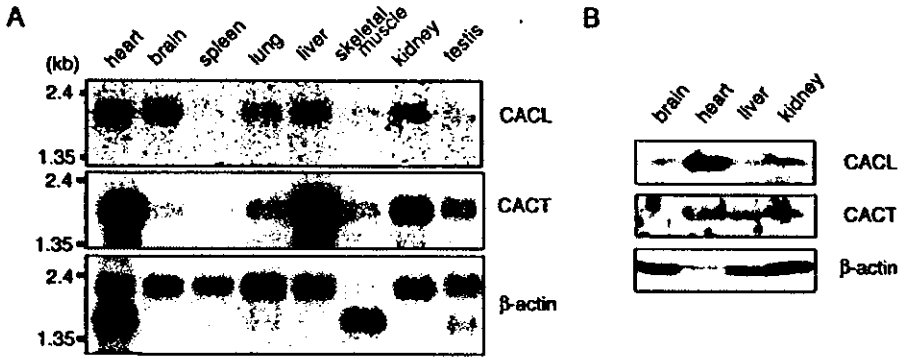

FIG. 2. **Expression of CACL in mouse tissues.** *A*, Northern blot analysis. A multiple tissue Northern blot filter (7762-1, Clontech) was hybridized with a probe corresponding to *mCACL* or *mCACT* cDNA. Each lane contains 2 μg of poly(A)$^+$ RNA. β-Actin cDNA (Clontech) was used as a control probe. Exposure time: 72 h for CACL and 24 h for CACT. *B*, Western blot analysis. An equal amount (100 μg/lane) of the protein lysates from various tissues was separated by SDS-PAGE, followed by Western blot analysis using antibodies against CACL, CACT, and β-actin.

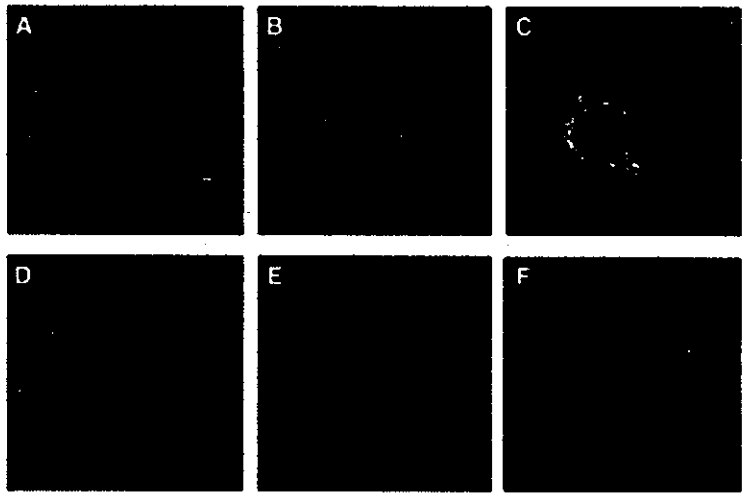

FIG. 3. **CACL is localized to mitochondria.** NIH3T3 cells overexpressing CACL with (*A–C*) or without (*D–F*) the myc-His$_6$ tag at the carboxyl terminus were fixed and subjected to immunostaining using the anti-His$_6$ or the anti-CACL antibody. Confocal images of anti-His$_6$ (*A*) and anti-CACL (*D*) staining (*green*), as well as images of mitochondria staining (*red*; *B* and *E*) with a fluorescent marker Mitotracker (Molecular Probes) are shown. Images were superimposed (*C* and *F*) using PhotoShop 5.0 (Adobe Systems Inc.).

the oleate plate (Fig. 4*C*), suggesting that the CACL protein possesses an enzymatic activity similar to Crc1p.

To examine more directly whether CACL possesses activity similar to that of CACT, we performed a biochemical assay for the acylcarnitine transporting activity of mitochondrial fractions using palmitoyl-[^{14}C]carnitine (16). To this end, we constructed NIH3T3 cells in which *CACL* or *CACT* was overexpressed under the control of the retroviral LTR promoter (Fig. 4*D*). As shown in Fig. 4*E*, liberation of [^{14}C]carnitine, which was produced enzymatically from palmitoyl-[^{14}C]carnitine in the mitochondrial matrix, was observed in the mitochondrial fractions harvested from cells infected with a control vector, and the activity was significantly elevated in cells overexpressing either *CACL* or *CACT*.

Moreover, we constructed a plasmid for the functional expression of the mCACL-His$_6$ fusion protein in *E. coli*. Cells harboring the plasmid expressed the recombinant protein in an arabinose-dependent manner (Fig. 4*F*), and the expression of mCACL conferred palmitoylcarnitine uptake activity to *E. coli* cells (Fig. 4*G*). Collectively, these data demonstrate that *CACL* indeed encodes a protein with acylcarnitine transporting activity in mitochondria.

Induction of CACL after Partial Hepatectomy and Fasting—As described above, *CACL* was found as a gene whose expression was up-regulated after PH in rats. We addressed whether *CACL* expression was altered in mouse livers after PH.

As shown in Fig. 5*A*, the expression level of the *CACL* transcript in the liver before the operation was low, and was increased at 6–12 h after PH (Fig. 5*A*, *left*). The *CACL* transcript level was slightly increased in sham-operated mice at 6 h (Fig. 5*A*, *right*). Consistently, the amount of the CACL protein was increased at 12 h after PH, whereas the increase was slight after the sham operation (Fig. 5, *B* and *C*). In contrast, a modest increase in *CACT* expression was observed, but its protein level was not increased significantly (Fig. 5, *A–C*). The hepatic surgeries did not affect the protein levels of CACL and CACT in other tissues such as heart (Fig. 5*D*).

Fasting is a stress that is known to cause a metabolic shift to preferentially use free fatty acids. We found that the transcript corresponding to *CACL* was induced markedly in liver after 12 h of fasting (Fig. 6*A*). *CACT* mRNA was also increased under the same condition (Fig. 6*A*). We further examined the amount of CACL protein in several tissues by Western blot analysis using the anti-CACL antibody. As shown in Fig. 6, *B–D*, the protein levels of CACL after fasting were markedly elevated in liver, and increased modestly in heart. In contrast, up-regulation was slight in kidney. We also observed an increase in the amount of CACT in livers and hearts after fasting. These data indicate that the expression of *CACL* and *CACT* is regulated by fasting in a tissue-specific manner and suggest that the induction of these carnitine carriers may contribute to a metabolic change in specific tissues such as the liver.

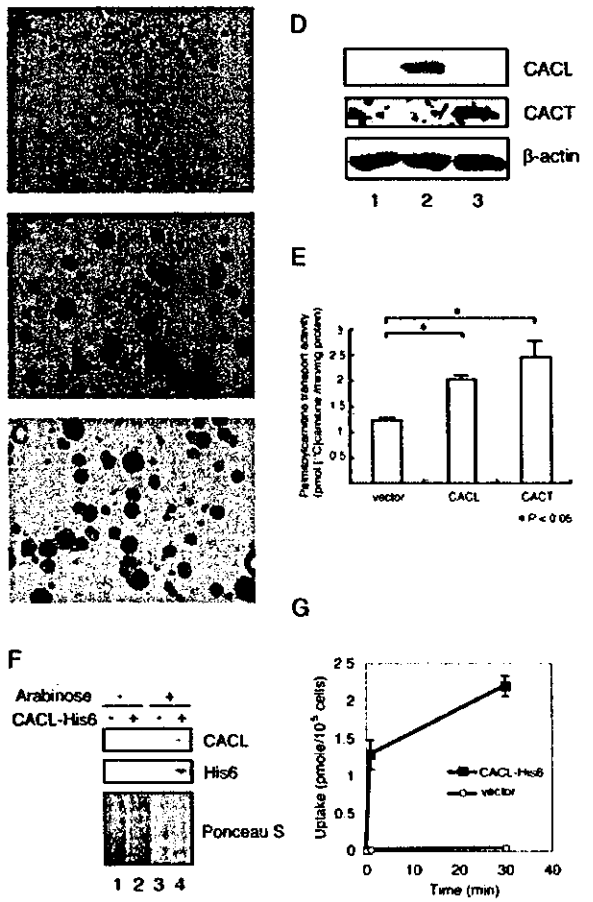

FIG. 4. **CACL possesses acylcarnitine importing activity.** *A–C*, rescue of the growth impairment of the yeast *Δcit2 Δcrc1* mutant on oleate by the expression of Crc1p or mCACL. The *Δcit2 Δcrc1* cells were transformed with control vector pRS316 (*A*), p316CRC1 (*B*), or pKT10-mCACL (*C*), and the transformants were grown in minimal medium containing 0.3% glucose for 24 h. The cultures were diluted with H_2O and spread onto agar plates of minimal oleate medium. Photographs were taken after incubation for 5 days at 30 °C. *D*, establishment of cells overexpressing *CACL* or *CACT*. NIH3T3 cells were infected with pMXpuro/mCACL (*lane 2*), pMXpuro/mCACT (*lane 3*), or a control vector pMXpuro (*lane 1*), and stable infectants were selected. Cell lysates (100 μg/lane) were analyzed by Western blot analysis using antibodies against mCACL, CACT, and β-actin. *E*, acylcarnitine transport activity in the mitochondrial fraction. Mitochondrial fractions were prepared and used for the acylcarnitine transport assay with palmitoyl-[^{14}C]carnitine (NEC-667, PerkinElmer Life Sciences) as described under "Experimental Procedures." The data presented are average ± S.D. of three independent experiments. *F–G*, functional expression of mCACL in *E. coli*. *E. coli* cells possessing pBAD/CACL-His$_6$ (*lanes 2* and *4*) or a control vector pBAD/gIIIA (*lanes 1* and *3*) were grown in the presence (*lanes 3* and *4*) or absence (*lanes 1* and *2*) of 0.2% arabinose for 18 h at 30 °C. Lysates were subjected to Western blot analysis using anti-CACL or anti-His$_6$ antibodies (*F*). In *G*, *E. coli* cells grown in LB + 0.2% arabinose were incubated with palmitoyl-[^{14}C]carnitine, and the incorporation of ^{14}C into cells at 30 °C was measured as described under "Experimental Procedures." The data presented are average ± S.D. of three independent experiments.

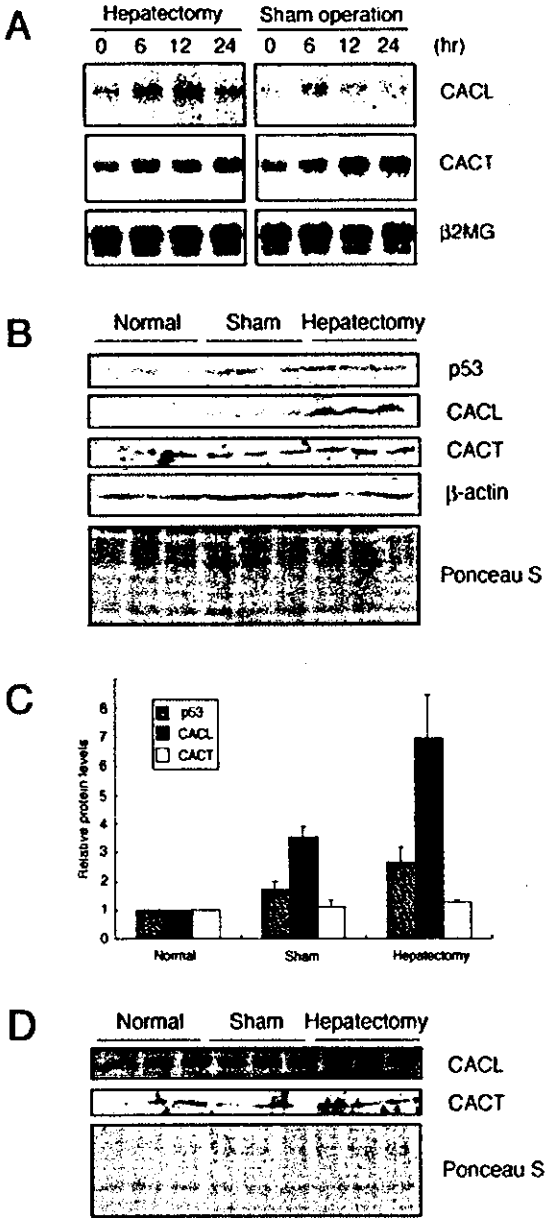

FIG. 5. **Induction of CACL after partial hepatectomy.** *A*, Northern blot analysis. A 70% hepatectomy was performed at time 0, and the remnant regenerating livers were collected at the indicated times after surgery. Livers were also collected from sham-operated C57BL/6 mice. Poly(A)$^+$ RNAs (5 μg/lane) were subjected to Northern blot analysis with *mCACL*, *mCACT*, and β_2-microglobulin cDNA probes. *B* and *C*, Western blot analysis of liver lysates. Livers were collected from three mice without operations and from mice 12 h after the hepatectomy or a sham operation. Postnuclear lysates were subjected to Western blot analysis using antibodies against p53, mCACL, CACT, and β-actin. In *C*, protein levels were quantitatively measured, and normalized -fold induction after the operations was calculated. Values shown are average ± S.D. for three different mice. Note that the protein levels of p53 increased after the partial hepatectomy, as reported previously (35). *D*, Western blot analysis of heart lysates. Hearts were collected at the same time points as in *B*, and postnuclear lysates were subjected to Western blot analysis.

DISCUSSION

In the present study we identified CACL, a novel mammalian protein that is localized to mitochondria and exhibits acylcarnitine transporting activity. The *CACL* transcript was found in tissues such as heart and liver, where its homologue *CACT* was expressed at a high level. In humans, patients with a CACT deficiency exhibited various cardiac symptoms and abnormal liver functions (7–9). Thus, CACL may not be able to compensate for CACT function in fatty acid metabolism of these tissues.

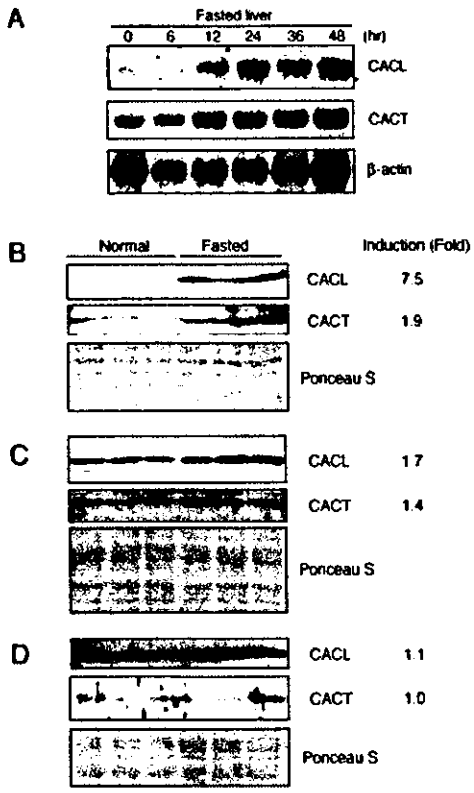

FIG. 6. **Induction of CACL after fasting.** *A*, Northern blot analysis. Mice that fasted for the indicated times were sacrificed, and poly(A)$^+$ RNAs were collected from the livers. Northern blot analysis was performed with probes for *mCACL* mRNA, *mCACT* mRNA, and β-actin mRNA. Each lane contained 10 μg of poly(A)$^+$ RNA. *B–D*, Western blot analysis. Protein lysates were prepared from the tissues of three mice before or after a 48-h fast. Western blot analysis was performed using antibodies against CACL and CACT. Each lane contained 100 μg of protein. Protein levels were quantitatively measured, and normalized -fold induction after fasting was calculated. Values shown are average for three different mice. Tissues examined were as follows: *B*, liver; *C*, heart; and *D*, kidney.

In contrast, the brain is a unique organ in which *CACL* is expressed at higher levels than is *CACT*. Although peroxisomal β-oxidation enzymes are expressed in brain (19), there have been no reports to show that the mitochondrial β-oxidation pathway is operating in the brain. The presence of the *CACL* transcript suggests that acylcarnitine might be used in this organ. The brain contains relatively high amounts of long-chain polyunsaturated fatty acids, such as docosahexaenoic acid, which are critical for its functions (20). It was recently reported that a novel carnitine palmitoyltransferase was expressed specifically in brain and testis (21) and that carnitine transporters on the plasma membrane, which are involved in carnitine uptake, were expressed in brain (22). Together with the carnitine-handling enzymes expressed in brain, CACL might have specialized roles in the metabolism of a distinct class of fatty acids that are involved in brain function.

The liver is a unique organ with a regenerative capacity. After 70% of the mass is surgically removed, the residual hepatic lobes enlarge to restore the original mass within 7 days, and vascularization is completed within the subsequent 7 days (23). A variety of genes are involved in the whole process of liver regeneration, although the molecular mechanisms underlying the process remain unknown. Recently, Su *et al.* (24) reported a microarray-based study of the gene expression profile during the priming phase of liver regeneration in mice. They reported up-regulation of phosphoenolpyruvate carboxykinase and glucose 6-phosphatase, which are involved in maintaining glucose levels after an acute loss of liver mass. Thus, a subtle regulation that switches energy metabolism appears to occur in the regenerating liver.

Carnitine has been thought to be one of the key factors in the regulation of liver regeneration, because the carnitine content in the liver increases after PH (25) and liver regeneration is accelerated by the administration of carnitine to hepatectomized rats (26). In addition, increases in the mRNA levels of carnitine palmitoyltransferase I and II have been observed in regenerating livers (27). Taken together, these results suggest that the carnitine-dependent pathway is important for energy supply when the liver, a major organ critical to maintaining metabolic and biosynthetic homeostasis, is partially removed. In agreement with this notion, we found that the level of CACL protein was elevated after PH. This acylcarnitine carrier may be involved in one of the key steps that regulate cellular metabolism during liver regeneration.

A change in the energy source from glucose to free fatty acids has been widely observed as an adaptive response to fasting (28). In the fasting heart, intracellular droplet accumulation was observed (29), and the content of glycerides and glycogen was increased through the inhibition of the glycolytic pathway and the enhancement of the β-oxidation pathway (30). A recent study using oligonucleotide microarrays revealed that the expression of a wide range of cardiac genes was affected by fasting, including the up-regulation of genes for fatty acid oxidation and gluconeogenesis and the down-regulation of genes for glycolysis (31). We found that *CACL* and *CACT* were up-regulated at the mRNA level in liver, and furthermore, fasting increased the amount of the CACL and CACT proteins in heart and liver. These two organs are prominent in the use of fatty acids upon starvation; fasted cardiac muscles directly use fatty acids as an energy source, whereas hepatic metabolism of fatty acids is mostly directed toward the synthesis of ketone bodies for use as energy sources in tissues such as brain (32). Thus, the up-regulation of CACL and CACT may contribute to the adaptation of the whole body to fasting.

Systemic energy metabolism has been shown to be tightly regulated by the action of hormones, and a disruption of this coordinated regulation causes disorders such as obesity and diabetes (33). Further studies of the coordinating mechanisms of glucose and lipid metabolism in the responsible organs will provide insights for the development of novel approaches to therapy or prevention of these disorders.

Acknowledgments—We thank Dr. Yoshiyuki Takahara (Ajinomoto Co., Inc.) for providing the microarray data, Dr. Toshio Kitamura for plasmids, Dr. V. A. Zammit for antibodies, and Dr. Satoshi Kametaka (Osaka University) for technical advice. We are grateful to Eiji Hayashi, Makoto Kimura, and Yayoi Tanaka (National Institute for Longevity Sciences) for technical assistance and to members of the Department of Geriatric Research for helpful discussions.

REFERENCES

1. Wallis, J. G., Watts, J. L., and Browse, J. (2002) *Trends Biochem. Biosci.* **27**, 467–473
2. Hale, D. E., and Bennett, M. J. (1992) *J. Pediatr.* **121**, 1–11
3. Pande, S. V. (1975) *Proc. Natl. Acad. Sci. U. S. A.* **72**, 883–887
4. Ramsay, R. R., Gandour, R. D., and van der Leij, F. R. (2001) *Biochim. Biophys. Acta* **1546**, 21–43
5. Indiveri, C., Iacobazzi, V., Giangregorio, N., and Palmieri, F. (1997) *Biochem. J.* **321**, 713–719
6. Huizing, M., Iacobazzi, V., Ijlst, L., Savelkoul, P., Ruitenbeek, W., van den Heuvel, L., Indiveri, C., Smeitink, J., Trijbels, F., Wanders, R., and Palmieri, F. (1997) *Am. J. Hum. Genet.* **61**, 1239–1245
7. Stanley, C. A., Hale, D. E., Berry, G. T., Deleeuw, S., Boxer, J., and Bonnefont, J. P. (1992) *N. Engl. J. Med.* **327**, 19–23
8. Pande, S. V., Brivet, M., Slama, A., Demaugre, F., Aufrant, C., and Saudubray, J. M. (1993) *J. Clin. Invest.* **91**, 1247–1252
9. Pande, S. V. (1999) *Am. J. Med. Sci.* **318**, 22–27

10. Higgins, G. M., and Anderson, R. M. (1931) *Arch. Pathol.* **12,** 186–202
11. Onishi, M., Kinoshita, S., Morikawa, Y., Shibuya, A., Phillips, J., Lanier, L. L., Gorman, D. M., Nolan, G. P., Miyajima, A., and Kitamura, T. (1996) *Exp. Hematol.* **24,** 324–329
12. Tanaka, K., Nakafuku, M., Tamanoi, F., Kaziro, Y., Matsumoto, K., and Toh-e, A. (1990) *Mol. Cell. Biol.* **10,** 4303–4313
13. Sikorski, R. S., and Hieter, P. (1989) *Genetics* **122,** 19–27
14. Fraser, F., and Zammit, V. A. (1999) *FEBS Lett.* **445,** 41–44
15. van Roermund, C. W. T., Hettema, E. H., van den Berg, M., Tabak, H. F., and Wanders, R. J. A. (1999) *EMBO J.* **18,** 5843–5852
16. Murthy, M. S., and Pande, S. V. (1984) *J. Biol. Chem.* **259,** 9082–9089
17. De Lucas, J. R., Dominguez, A. I., Valenciano, S., Turner, G., and Laborda, F. (1999) *Arch. Microbiol.* **171,** 386–396
18. van Roermund, C. W. T., Elgersma, Y., Singh, N., Wanders, R. J. A., and Tabak, H. F. (1995) *EMBO J.* **14,** 3480–3486
19. Knoll, A., Sargueil, F., Salles, J., Cassagne, C., and Garbay, B. (1999) *Brain Res. Mol. Brain Res.* **74,** 217–220
20. Uauy, R., Hoffman, D. R., Peirano, P., Birch, D. G., and Birch, E. E. (2001) *Lipids* **36,** 885–895
21. Price, N. T., van der Leij, F. R., Jackson, V. N., Corstorphine, C. G., Thomson, R., Sorensen, A., and Zammit, V. A. (2002) *Genomics* **80,** 433–442
22. Eraly, S., and Nigam, S. (2002) *Biochem. Biophys. Res. Commun.* **297,** 1159–1166
23. Michalopoulos, G. K., and DeFrances, M. C. (1997) *Science* **276,** 60–66
24. Su, A. I., Guidotti, L. G., Pezacki, J. P., Chisari, F. V., and Schultz, P. G. (2002) *Proc. Natl. Acad. Sci. U. S. A.* **99,** 11181–11186
25. Lai, H. S., Chen, Y., and Chen, W. J. (1998) *World J. Surg.* **22,** 42–46; 46–47
26. Holecek, M., Simek, J., Zadak, Z., and Blaha, V. (1989) *Physiol. Bohemoslov* **38,** 503–508
27. Asins, G., Rosa, J. L., Serra, D., Gil-Gomez, G., Ayte, J., Bartrons, R., Tauler, A., and Hegardt, F. G. (1994) *Biochem. J.* **299,** 65–69
28. Neely, J. R., and Morgan, H. E. (1974) *Annu. Rev. Physiol.* **36,** 413–459
29. Adams, M. G., Barer, R., Joseph, S., and Om'Iniabohs, F. (1981) *J. Pathol.* **135,** 111–126
30. Denton, R. M., and Randle, P. J. (1967) *Biochem. J.* **104,** 416–422
31. Suzuki, J., Shen, W. J., Nelson, B. D., Selwood, S. P., Murphy, G. M., Jr., Kanefara, H., Takahashi, S., Oida, K., Miyamori, I., and Kraemer, F. B. (2002) *Am. J. Physiol.* **283,** E94–E102
32. Mitchell, G. A., Kassovska-Bratinova, S., Boukaftane, Y., Robert, M. F., Wang, S. P., Ashmarina, L., Lambert, M., Lapierre, P., and Potier, E. (1995) *Clin. Invest. Med.* **18,** 193–216
33. Saltiel, A. R., and Kahn, C. R. (2001) *Nature* **414,** 799–806
34. Kyte, J., and Doolittle, R. F. (1982) *J. Mol. Biol.* **157,** 105–132
35. Inoue, Y., Tomiya, T., Yanase, M., Arai, M., Ikeda, H., Tejima, K., Ogata, I., Kimura, S., Omata, M., and Fujiwara, K. (2002) *Hepatology* **36,** 336–344

Available online at www.sciencedirect.com
SCIENCE DIRECT®
Gene 310 (2003) 17–28
GENE
AN INTERNATIONAL JOURNAL ON GENES AND GENOMES
www.elsevier.com/locate/gene

Characterization of the mouse *Abcc12* gene and its transcript encoding an ATP-binding cassette transporter, an orthologue of human ABCC12☆

Hidetada Shimizu[a], Hirokazu Taniguchi[b], Yoshitaka Hippo[b], Yoshihide Hayashizaki[c], Hiroyuki Aburatani[b], Toshihisa Ishikawa[a,*]

[a]*Department of Biomolecular Engineering, Graduate School of Bioscience and Biotechnology, Tokyo Institute of Technology, Nagatsuta 4259, Midori-ku, Yokohama 226-8501, Japan*
[b]*Genome Science Division, Research Center for Advanced Science and Technology, The University of Tokyo, 4-6-1 Komaba, Meguro-ku, Tokyo 153-8904, Japan*
[c]*Genome Exploration Research Group, Genome Science Laboratory, Genome Sciences Center, RIKEN, 1-7-22 Suehiro-cho, Tsurumi-ku, Yokohama 230-0045, Japan*

Received 13 December 2002; received in revised form 24 February 2003; accepted 6 March 2003
Received by T. Gojobori

Abstract

We have recently reported on two novel human ABC transporters, ABCC11 and ABCC12, the genes of which are tandemly located on human chromosome 16q12.1 [Biochem. Biophys. Res. Commun. 288 (2001) 933]. The present study addresses the cloning and characterization of Abcc12, a mouse orthologue of human ABCC12. The cloned Abcc12 cDNA was 4511 bp long, comprising a 4101 bp open reading frame. The deduced peptide consists of 1367 amino acids and exhibits high sequence identity (84.5%) with human ABCC12. The mouse *Abcc12* gene consists of at least 29 exons and is located on the mouse chromosome 8D3 locus where conserved linkage homologies have hitherto been identified with human chromosome 16q12.1. The mouse *Abcc12* gene was expressed at high levels exclusively in the seminiferous tubules in the testis. In addition to the Abcc12 transcript, two splicing variants encoding short peptides (775 and 687 amino acid residues) were detected. In spite of the genes coding for both ABCC11 and ABCC12 being tandemly located on human chromosome 16q12.1, no putative mouse orthologous gene corresponding to the human *ABCC11* was detected at the mouse chromosome 8D3 locus.

Keywords: ATP binding cassette transporter; Mouse; Abcc12; Mouse chromosome 8; Human chromosome 16; Sertoli cell

1. Introduction

The ATP-binding cassette (ABC) transporters form one of the largest protein families and play a biologically important role as membrane transporters or ion channel modulators (Higgins, 1992). According to the recently published draft sequence of the human genome, more than 50 human ABC transporter genes (including pseudogenes[1]) are anticipated to exist in the human genome. Hitherto 49 human ABC-transporter genes have been identified and sequenced (recent reviews: Klein et al., 1999; Dean et al., 2001; Borst and Oude Elferink, 2002). Based on the arrangement of their molecular structural components, i.e. the nucleotide binding domain and the topology of transmembrane spanning domains, human ABC transporters are classified into seven different gene families designated as A to G (the new nomenclature of human ABC transporter genes: http://gene.ucl.ac.uk/nomenclature/genefamily/abc.html). Mutations in the human ABC transporter genes have been reported to cause such genetic diseases as Tangier

☆ The cDNA sequences of mouse Abcc12 and its splice variants A and B have been registered in GenBank under the accession numbers of AF502146 (April 12, 2002), AF514414 (May 22, 2002), and AF514415 (May 22, 2002), respectively.

Abbreviations: ABC, ATP-binding cassette; EST, expresed sequence tag; MRP, multidrug resistance-associated protein; GAPDH, glutaraldehyde dehydrogenase; GS-X, pump, ATP-dependent glutathione *S*-conjugate export pump; RT–PCR, reverse transcriptase–polymerase chain reaction.

* Corresponding author. Tel.: +81-45-924-5800; fax: +81-45-924-5838.
E-mail address: tishikaw@bio.titech.ac.jp (T. Ishikawa).

[1] A truncated human ABC transporter, ABCC13 (GenBank accession number: AF418600), has most recently been cloned (Yabuuchi et al., 2002).

0378-1119/03/$ - see front matter © 2003 Elsevier Science B.V. All rights reserved.
doi:10.1016/S0378-1119(03)00504-3

disease, cystic fibrosis, Dubin–Johnson syndrome, Stargardt disease, and sitosterolemia (recent reviews: Dean et al., 2001; Borst and Oude Elferink, 2002).

We originally reported that transport of glutathione S-conjugates and leukotriene C_4 (LTC_4) across the cell membrane is mediated by an ATP-dependent transporter named the 'GS-X pump' (Ishikawa, 1989, 1992); however, the molecular nature of the transporter was not uncovered at that time. Later studies have provided evidence that the GS-X pump is encoded, at least, by the ABCC1 (MRP1) gene (Leier et al., 1994; Müller et al., 1994). ABCC1 (MRP1) was first identified by Cole et al. (1992) in the molecular cloning of cDNA from human multidrug-resistant lung cancer cells. After the discovery of the ABCC1 (MRP1) gene, six human homologues, ABCC2 (cMOAT/MRP2), ABCC3 (MRP3), ABCC4 (MRP4), ABCC5 (MRP5), ABCC6 (MRP6), and ABCC10 (MRP7) have been successively identified. Those ABC transporters exhibit a wide spectrum of biological functions and are involved in the transport of drugs as well as endogenous substances (see recent reviews: Borst and Oude Elferink, 2002; Ishikawa, in press).

Most recently, our group (Yabuuchi et al., 2001) and others (Tammur et al., 2001; Bera et al., 2001, 2002) have independently discovered two novel ABC transporters, human ABCC11 (MRP8) and ABCC12 (MRP9), that belong to the ABCC gene family. The predicted amino acid sequences of both gene products show a high similarity with ABCC5. The *ABCC11* and *ABCC12* genes consist of at least 30 and 29 exons, respectively, and they are tandemly located in a tail-to-head orientation on human chromosome 16q12.1 (Yabuuchi et al., 2001; Tammur et al., 2001). The physiological functions of these genes are not yet known; however recent linkage analyses have demonstrated that a putative gene responsible for paroxysmal kinesigenic choreoathetosis (PKC), a genetic disease of infancy, is located in the region of 16p11.2–q12.1 (Lee et al., 1998; Tomita et al., 1999). Since the *ABCC11* and *ABCC12* genes are encoded at that 16q12.1 locus, a potential link between the PKC gene and these ABC transporters has been implicated.

To elucidate the physiological function of human ABCC11 and ABCC12, knockout mice are considered to be a useful animal model. For this reason, we have undertaken the present study to pursue mouse orthologues of ABCC11 and ABCC12. In this study, we have cloned the cDNA of mouse Abcc12 and characterized its chromosomal location, gene organization, tissue-specific expression, the putative protein structure, and splicing variants.

2. Materials and methods

2.1. Cloning of mouse Abcc 12 cDNA

Mouse EST clones bearing a high similarity to partial sequences of human ABCC 12 cDNA were extracted from the NCBI mouse EST database and the mouse cDNA 'FANTOM 2' database of RIKEN (The FANTOM Consortium, 2002) by using the NCBI BLAST search program (Fig. 1). We have screened multiple tissue cDNA libraries (MTC, Clontech, Palo Alto, CA, USA) by PCR with the following primers deduced from the EST sequences: the forward primer, 5′-AGTTCCCTCATTTCAGCTCTCC-TAGGAC-3′, and the backward primer, 5′-GCAGGTA-GAGCTGACGATTAGCATAC-3′. High expression was detected in mouse testis.

To clone the mouse Abcc12 cDNA from the testis, we have designed four sets of PCR primers, as shown in Fig. 1. The PCR primer sets were as follows: c12-1 (the forward primer: 5′-GCCAAAAGTCGAGGGCTCCAAAACACC-3′ and the backward primer: 5′-GGCCACTGCTTTGACC-GAGAA-3′), c12-2 (the forward primer: 5′-GGCTGGC-TATGTCCAAAGTGGAA-3′ and the backward primer: 5′-GATGCCAAACATCAACACAGACACC-3′), c12-3 (the forward primer: 5′-GATGATGGGCAGCTCTGCTT-TC-3′ and the backward primer: 5′-TCACATGTCCA-TCGCCTCCTCTCA-3′), and c12-4 (the forward primer: 5′- GCCCGACTCTGCATTTGCGA-3′ and the backward primer: 5′-CAAAATCCAGGAACGCTGTCATCTCC-3′). The PCR reaction was performed with mouse testis cDNA (Clontech) and *Ex Taq* polymerase (TaKaRa, Japan), where the reaction consisted of 30 cycles of 95 °C for 30 s, 58 °C for 30 s, and 72 °C for 90 s. After agarose gel electrophoresis, the PCR products were extracted from the gels and subsequently inserted into TA cloning vectors (Invitrogen, Japan). The sequences of the inserts were analyzed with an automated DNA sequencer. (Toyobo Gene Analysis, Japan). The whole cDNA of mouse Abcc12 was obtained by assembling those partial sequences.

2.2. Detection of mouse Abcc 12 transcripts by PCR in different tissues

The expression of mouse Abcc 12 in different organs was examined by PCR with the mouse Multiple Tissue cDNA (MTC, Clontech). Two sets of PCR primers were designed to detect the corresponding transcript (Fig. 1), namely, the primer set #1 detecting the 5′-part of Abcc12 cDNA (the forward primer: 5′-CCACTGTCTCCTTATGACTCATCG-GAC-3′, the backward primer: 5′-GGGACAAAACAAGG-CAGCCTCAAAC-3′) and the primer set #2 recognizing the 3′-part of Abcc12 cDNA (the forward primer: 5′-TAT-GGCCCGGGCACTTCTCCGTAA-3′, the backward primer 5′-GACCTTTACAGTCCAACCTCTGCAGCTAGT-3′). The PCR reaction consisted of 35 cycles of 95 °C for 30 s, 58 °C for 30 s, and 72 °C for 30 s. The reaction products were detected by agarose gel electrophoresis.

2.3. Northern blot analysis

Mouse organs (i.e. heart, kidney, brain, testis, spleen, stomach, liver, thymus, and small intestine) were surgically

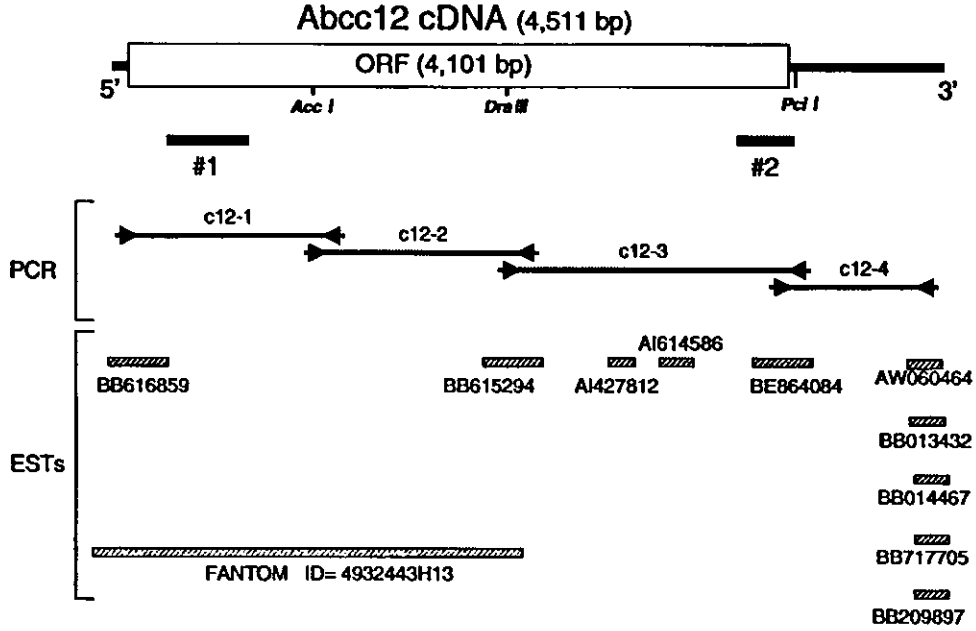

Fig. 1. Strategy for the cloning of mouse Abcc12 cDNA. The open reading frame (ORF) is indicated by a box. The cleavage sites by restriction enzymes (*Acc* I, *Dra* III and *Pci* I) are also indicated. The cDNA was cloned by PCR with four sets of primers, c12-1, c12-2, c12-3, and c12-4, as described in Section 2. The forward and backward PCR primers are indicated by arrows, and the resulting PCR products are represented by straight lines. ESTs and the FANTOM 2 cDNA are sorted according to the sequence homology with Abcc12 cDNA. PCR products used to detect the Abcc12 transcript in different tissues are indicated by #1 and #2.

excised from Balb/C mice (10 weeks old) under anesthesia and immediately frozen in liquid nitrogen. The tissue was pulverized in a mortar containing liquid nitrogen. The resulting tissue powder was subsequently homogenized in TRIzol (Invitrogen, Japan) by using a Polytron homogenizer, and total RNA was extracted according to the manufacturer's protocol. A sample (15 μg/lane as determined by absorbance at 260 nm) of RNA, thus prepared, was subjected to electrophoresis in 1% (w/v) agarose gels containing formaldehyde and then transferred to Hybond-XL membranes (Amersham Pharmacia Biotech). RNA was fixed on the membrane surface by baking at 80 °C for 2 h.

Three different DNA probes encoding partial sequences (463–1165; 1440–2116; 3660–4154) of the Abcc12 cDNA ORF were prepared and separately labeled with [^{32}P]dCTP by using the BcaBest labeling kit (TaKaRa) according to the random-primed labeling method. Hybridization with those DNA probes was carried out according to the hybridization protocol of the Expresshybri kit (Clontech), and the hybridization signal was detected in a BASS 2000 (Fuji Film, Japan).

2.4. Laser-captured microdissection and RT–PCR

The frozen tissue of mouse testis was cut into thin sections (5 μm thickness) with a microtome (Leika GmbH, Germany) and mounted onto glass slides. The tissue slice on the glass slide was stained in 70% Giemsa solution. After staining, the tissue slices were dehydrated in 100% ethanol and subsequently in 100% xylene. The slide was air-dried, and the seminiferous tubules and the interstitium in the tissue slices were excised by laser-capture microdissection with an Arcturus PixCell 2 LCM system (Arcturus Engineering, Mountain View, CA). The dissected samples were homogenized in 200 μl of TRIzol, and RNA was extracted. mRNA was then converted to cDNA by reverse transcriptase (RT) using a SensiScripts kit (Qiagen). Expression of mouse Abcc12 in these samples was detected by PCR with the same primers and under the same conditions as described in Section 2.2.

2.5. In situ hybridization

The testis was surgically excised from mice under anesthesia and immersed in phosphate-buffered saline (PBS) containing 4% paraformaldehyde. The tissue was embedded in paraffin, and thin sections (4 μm thickness) were prepared with a microtome. The resulting thin sections were soaked in xylene three times (3 min for each) and twice in 100% ethanol (3 min for each). Thereafter, sections were rinsed in 70% ethanol and subsequently in 0.1% DEPC-treated water three times. Prior to hybridization, the sections were treated with proteinase K (1:400 v/v) in Tris-buffered saline (TBS) at room temperature for 10 min and

A

```
Mouse Abcc12     1 MVGEGPYLISDLDRRGHRRSFAERYDPSLKTMIPVRPRARLAPNPVDDAGLLSFATFSWL 60
Human ABCC12     1 MVGEGPYLISDLDQRGRRRSFAERYDPSLKTMIPVRPCARLAPNPVDDAGLLSFATFSWL 60

Mouse Abcc12    61 TPVMIRSYKHTLTVDTLPPLSPYDSSDINAKRFQILWEEEIKRVGPEKASLGRVVWKFQR 120
Human ABCC12    61 TPVMVKGYRQRLTVDTLPPLSTYDSSDTNAKRFRVLWDEEVARVGPEKASLSHVVWKFQR 120

Mouse Abcc12   121 TRVLMDVVANILCIVMAALGPTVLIHQILQHITSISSGHIGIGICLCLALFTTEFTKVLF 180
Human ABCC12   121 TRVLMDIVANILCIIMAAIGPTVLIHQILQQTERTSG-KVWVGIGLCIALFATEFTKVFF 179

Mouse Abcc12   181 WALAWAINYRTAIRLKVALSTLIFENLLSFKTLTHISAGEVLNILSSDSYSLFEAALFCP 240
Human ABCC12   180 WALAWAINYRTAIRLKVALSTLVFENLVSFKTLTHISVGEVLNILSSDSYSLFEAALFCP 239

Mouse Abcc12   421 PPSYITQPEDPDTILLLANATLTWEQEINRKSDPPKAQIQKRHVFKKQRPELYSEQSRSD 480
Human ABCC12   420 PPSYITQPEDPDTVLLLANATLTWEHEARQESTPKKLQNQKRHLCKKQRSEAYSERSPPA 479
                                                  Walker A
Mouse Abcc12   481 QGVASPEWQSGSPKSVLHNISFVVRKGKVLGICGNVGSGKSSLISALLGQMQLQKGVVAV 540
Human ABCC12   480 KGATGPEEQSDSLKSVLHSISFVVRKGKILGICGNVGSGKSSLLAALLGQMQLQKGVVAV 539

Mouse Abcc12   541 NGPLAYVSQQAWIFHGNVRENILFGEKYNHQRYQHTVHVCGLQKDLNSLPYGDLTEIGER 600
Human ABCC12   540 NGTLAYVSQQAWIFHGNVRENILFGEKYDHQRYQHTVRVCGLQKDLSNLPYGDLTEIGER 599
                        Signature C      Walker B
Mouse Abcc12   601 GVNLSGGQRQRISLARAVYANRQLYLLDDPLSAVDAHVGKHVFEECIKKTLRGKTVVLVT 660
Human ABCC12   600 GLNLSGGQRQRISLARAVYSDRQLYLLDDPLSAVDAHVGKHVFEECIKKTLRGKTVVLVT 659

Mouse Abcc12   661 HQLQFLESCDEVILLEDGEICEKGTHKELMEERGRYAKLIHNLRGLQFKDPEHIYNVAMV 720
Human ABCC12   660 HQLQFLESCDEVILLEDGEICEKGTHKELMEERGRYAKLIHNLRGLQFKDPEHLYNAAMV 719

Mouse Abcc12   721 ETLKESPAQRDEDAVLASGDEKDEGKEPETEE-FVDTRAPAHQLIQTESPQEGIVTWKTY 779
Human ABCC12   720 EAFKESPAEREEDAVLAPGNEKDEGKESETGSEFVDTKVPEHQLIQTESPQEGTVTWKTY 779

Mouse Abcc12   780 HTYIKASGGYLVSFLVLCLFFLMMGSSAFSTWWLGIWLDRGSQVVCASQNNKTACNVDQT 839
Human ABCC12   780 HTYIKASGGYLLSLFTVFLFLLMIGSAAFSNWWLGLWLDKGSRMTCGPQGNRTMCEVGAV 839

Mouse Abcc12   840 LQDTKHHMYQLVYIASMVSVLMFGIIKGFTFTNTTLMASSSLHNRVFNKIVRSPMSFFDT 899
Human ABCC12   840 LADIGQHVYQRVYTASMVFMLVFGVTKGFVFTKTTLMASSSLHDTVFDKILKSPMSFFDT 899

Mouse Abcc12   900 TPTGRLMNRFSKDMDELDVRLPFHAENFLQQFFMVVFILVIMAAVFPVVLVVLAGLAVIF 959
Human ABCC12   900 TPTGRLMNRFSKDMDELDVRLPFHAENFLQQFFMVVFILVILAAVFPAVLLVVASLAVGF 959

Mouse Abcc12   960 LILLRIFHRGVQELKQVENISRSPWFSHITSSIQGLGVIHAYDKKDDCISKFKTLNDENS 1019
Human ABCC12   960 FILLRIFHRGVQELKKVENVSRSPWFTHITSSMQGLGIIHAYGKKESCIT-Y-------- 1010

Mouse Abcc12  1020 SHLLYFNCALRWFALRMDILMNIVTFVVALLVTLSFSSISASSKGLSLSYIIQLSGLLQV 1079
Human ABCC12  1011 -HLLYFNCALRWFALRMDVLMNILTFTVALLVTLSFSSISTSSKGLSLSYIIQLSGLLQV 1069

Mouse Abcc12  1080 CVRTGTETQAKFTSAELLREYILTCVPEHTHPFKVGTCPKDWPSRGEITFKDYRMRYRDN 1139
Human ABCC12  1070 CVRTGTETQAKFTSVELLREYISTCVPECTHPLKVGTCPKDWPSCGEITFRDYQMRYRDN 1129
                                  Walker A
Mouse Abcc12  1140 TPLVLDGLNLNIQSGQTVGIVGRTGSGKSSLGMALFRLVEPASGTIIIDEVDICTVGLED 1199
Human ABCC12  1130 TPLVLDSLNLNIQSGQTVGIVGRTGSGKSSLGMALFRLVEPASGTIFIDEVDICILSLED 1189

Mouse Abcc12  1200 LRTKLTMIPQDPVLFVGTVRYNLDPLGSHTDEMLWHVLERTFMRDTIMKLPEKLQAEVTE 1259
Human ABCC12  1190 LRTKLTVIPQDPVLFVGTVRYNLDPFESHTDEMLWQVLERTFMRDTTMKLPEKLQAEVTE 1249
                        Signature C      Walker B
Mouse Abcc12  1260 NGENFSVGERQLLCMARALLRNSKIILLDEATASMDSKTDTLVQSTIKEAFKSCTVLTIA 1319
Human ABCC12  1250 NGENFSVGERQLLCVARALLRNSKIILLDEATASMDSKTDTLVQNTIKDAFKGCTVLTIA 1309

Mouse Abcc12  1320 HRLNTVLNCDLVLVMENGKVIEFDKPEVLAEKPDSAFAMLLAAEVGL 1366
Human ABCC12  1310 HRLNTVLNCDHVLVMENGKVIEFDKPEVLAEKPDSAFAMLLAAEVRL 1356
```

Fig. 2. Alignments of the mouse Abcc12 and human ABCC12 proteins. (A) Amino acid sequences were aligned by using the GENETYX-MAC program. The Walker A and B motifs as well as the signature C are indicated by boxes. (B) The hydropathy plots of mouse Abcc12 (this study) and human ABCC12 (Yabuuchi et al., 2001). The hydropathy profiles were calculated according to the Kyte and Doolittle (1982) algorithm.

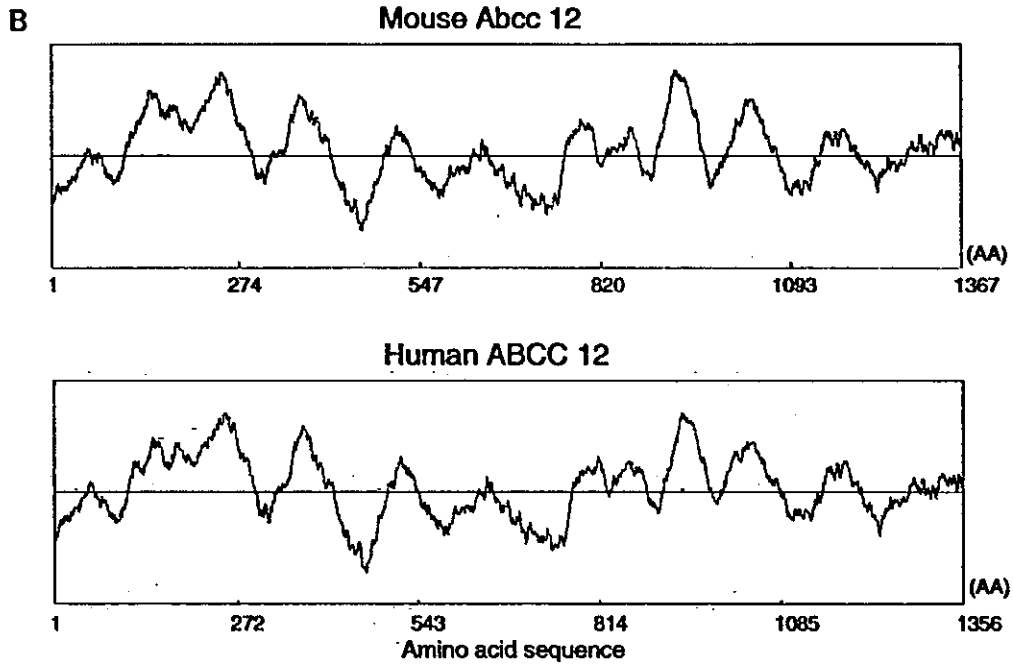

Fig. 2 (*continued*)

then rinsed with 0.1% DEPC-treated water. The following biotin-labeled oligonucleotide DNA probes were synthesized, i.e. the sense probe: 5′-AGCCTGACTCTGCATTTGCGATGTTACTAGCTGCAG-3′ and the anti-sense probe: 5′-CTGCAGCTAGTAACATCGCAAATGCAGAGTCAGGCT-3′. The probes were diluted in the DAKO in situ hybridization solution (DAKO S3304) at a final concentration of 1 ng/ml. The hybridization with the sense or the anti-sense probe was carried out on the thin section at 37 °C overnight. Thereafter, the slides were incubated in 0.1× SSC (300 mM sodium chloride and 1.5 mM sodium citrate, pH 7.0) at 37 °C for 20 min twice and washed in TBS at room temperature for 3 min.

In situ hybridization signals were visualized by a tyramide amplification signal detection system using the DAKO GenPoint system (DAKO K0620), according to manufacturer's instructions. Finally, the sections were counterstained with Mayer's hematoxylin (Sigma, USA).

2.6. Data analysis

DNA sequences were analyzed with the GENETYX-MAC software ver.11 and compared with other ABCC transporter genes registered in the NCBI database. The hydropathy profile of the protein deduced from the cDNA sequence was calculated with the Kyte and Doolittle hydropathy algorithm (Kyte and Doolittle, 1982), and the SOSUI program (http://sosui.proteome.bio.tuat.ac.jp/sosuimenu0.html) was used to predict transmembrane domains. Phylogenic relationships were calculated by using the distance-based neighbor-joining method (Saitou and Nei, 1987).

3. Results

3.1. Cloning and characterization of mouse Abcc 12 cDNA

Fig. 1 depicts the strategy of cloning mouse Abcc12 cDNA. The sequence of human ABCC12 cDNA was applied to the currently available mouse EST database on an NCBI BLAST search to discover ESTs encoding partial sequences of mouse Abcc 12. Thereby, the following EST clones were extracted: BB616859, BB615294, AI427812, AI614586, BE864084, AW060464, BB013432, BB014467, BB717705, and BB209897. In addition, in a search of the FANTOM 2 database of RIKEN, we found one cDNA clone (ID number = 4932443H13) that exhibited a high sequence homology with human ABCC12 cDNA. Based on those ESTs as well the partial cDNA clone (ID = 4932443H13), we designed four sets of PCR primers to clone the mouse Abcc12 cDNA (see Section 2 for experimental details). By PCR, we obtained a total of four cDNA fragments (Fig. 1) and assembled them to construct the full cDNA encoding mouse Abcc12.

Table 1
Amino acid sequence identity of the mouse Abcc 12 with human ABC proteins in the ABCC sub-family

ABC protein	Identity (%)
ABCC1	33.4
ABCC2	32.1
ABCC3	31.1
ABCC4	40.2
ABCC5	43.7
ABCC6	28.5
CFTR (ABCC7)	27.9
ABCC8	30.6
ABCC9	27.9
ABCC10	34.6
ABCC11	47.8
ABCC12	84.5

The amino acid sequences of human ABC proteins were acquired from the NCBI database (refer to the accession numbers given in the legend of Fig. 3).

3.2. Characterization of mouse Abcc12 cDNA in comparison with members of the human ABCC sub-family

The cloned mouse Abcc12 cDNA (GenBank accession number: AF502146) was 4511 bp long, containing a 4101 bp open reading frame (ORF). The Abcc12 cDNA has a Kozak consensus initiation sequence (Kozak, 1991) for translation around the first ATG region, namely, 5′-ATCAAGATGG-3′. The amino acid sequence deduced from the cDNA sequence with the GENETYX-MAC program revealed that the cDNA encodes a single peptide consisting of 1366 amino acid residues (Fig. 2A). Motif analysis predicted the existence of two sets of ATP-binding cassettes (Walker et al., 1982): namely, Walker A (amino acids 514–521 and 1161–1168), Walker B (amino acids 624–628 and 1284–1288), and signature C motifs (amino acids 604–618 and 1264–1278) (Fig. 2A). Fig. 2B shows the hydropathy plots of mouse Abcc12 and human ABCC12, demonstrating a remarkable similarity between these transporters.

Table 1 shows that the amino acid sequence of mouse Abcc12 has the highest identity with human ABCC12 among the hitherto known members of the human ABCC sub-family. The sequence identity of mouse Abcc12 with human ABCC12 was 84.5%, whereas its identity with human ABCC11 was 47.8%. The identity of mouse Abcc12 with other human members was relatively low, in the range of 27.9 to 43.7% (Table 1).

Fig. 3 shows the phylogenic relationship among the members of the human and mouse ABCC subfamily. Mouse Abcc12, as well as human ABCC12, apparently belongs to a cluster named 'Class D' that comprises ABCC4, ABCC5, ABCC11, Abcc4, and Abcc5 (see Section 4 for the classification).

3.3. Chromosomal location of the mouse Abcc 12 gene

Fig. 4 shows the location of the *Abcc12* gene on the mouse chromosome 8. The mouse Abcc12 gene spans a 65 kb length and is located between two microsatellite markers, D8Mit347 and D8Mit348, at the D3 region of the mouse chromosome 8 (Fig. 4), as referred to in the mouse genome databases of NCBI and EMBL/UCSC (Mouse Genome Sequencing Consortium, 2002). This genome region of the mouse chromosome 8 is reportedly related to human chromosome 16q12.1, where the human *ABCC11* and *ABCC12* genes are tandemly located (Yabuuchi et al., 2001; Tammur et al., 2001). Comparison of the cloned

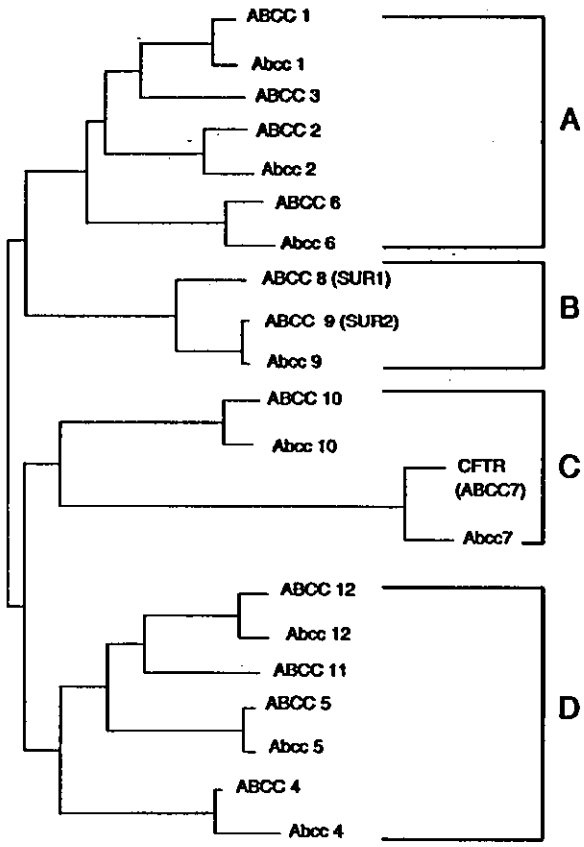

Fig. 3. The phylogenetic relationship among hitherto characterized members of the human and mouse ABCC sub-family. The phylogenetic distance was calculated according to the distance-based neighbor-joining method (Saitou and Nei, 1987). For the sequences of those ABC transporters, accession numbers are as follows: human ABCC1 (NM004996), ABCC2 (NM000392), ABCC3 (Y17151), ABCC4 (NM005845), ABCC5 (NM005688), ABCC6 (NM001171), ABCC7 (NM000492), ABCC8 (NM000352), ABCC9 (NM005691), ABCC10 (AK000002), ABCC11 (AF367202), ABCC12 (NM033226) mouse Abcc1 (NM008576), Abcc2 (NM013806), Abcc4 (D630049P08), Abcc5 (NM013790), Abcc6 (NM018795), Abcc7 (NM021050), Abcc8 (XM133448), Abcc9 (NM011511), Abcc10 (AF406642), Abcc12 (AF502146).

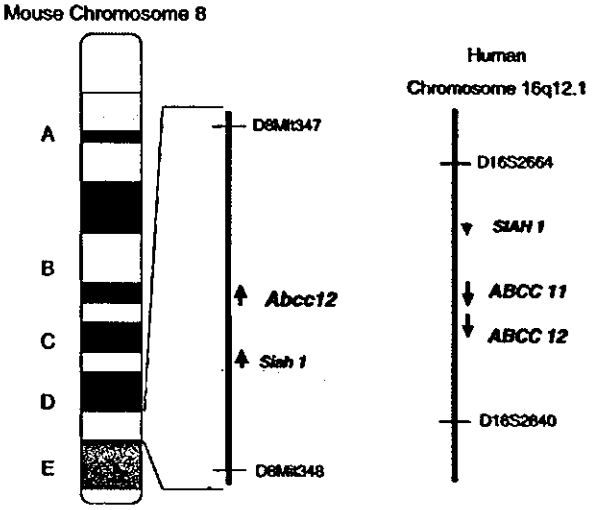

Fig. 4. Location of the *Abcc12* gene on mouse chromosome 8. *Abcc12* and *Siah 1* genes are located in the mouse chromosomal region between two microsatellite markers, D8Mit347 and D8Mit348. Human *ABCC11*, *ABCC12*, and *SIAH 1* genes are located in the region between D16S2664 and D16S2840 on the human chromosome 16q12.1.

Abcc12 cDNA with the mouse genome data revealed that the *Abcc12* gene consists of at least 29 exons, where the translation start codon (ATG) was found in exon 1. In addition, two sets of ATP-binding cassettes were detected. The first Walker A motif is located in the exon 10, whereas the second Walker A motif spreads over exons 24 and 25. Two Walker B motifs are encoded in exons 13 and 28, and two signature C motifs are located in exons 13 and 27.

Table 2 summarizes the exon and intron boundaries with partial sequences at each splicing site of the *Abcc12* gene; however, the partial sequences of the introns proximal to both 5′- and 3′-ends of exon 3 are presently not available (Table 2). These results suggest that the splicings of the mouse Abcc12 gene follow the conventional GT–AG rule, except for the exon 19.

3.4. Tissue-dependent expression of the mouse Abcc 12 gene

Fig. 5A shows the expression levels of the mouse Abcc12 gene in different organs as detected by RT–PCR with two different sets of PCR primers #1 and #2 (see Fig. 1 and Section 2 for details). The products of PCR reactions with primers #1 and #2 were 486 and 288 bp, respectively. Among the organs tested, the highest expression (mRNA) of

Table 2
Partial sequences of intron/exon and exon/intron boundaries in the mouse *Abcc 12* gene

Exon	Size (bp)	Intron/Exon		Exon/Intron	
1	152	tgtcccgaag	CCAAGAGTCG	CCCGTGCAAG	gtgagccagg
2	156	tttgctctag	GTTGGCACCC	ACGCCAAGAG	gtaccaggct
3[a]	147	nnnnnnnn	ATTCCAGATC	CTTGGGGCCG	nnnnnnnn
4	238	tgtttacag	ACAGTTCTCA	TGCAGGCGAG	gtaagcaggg
5	174	ttctttctag	GTACTCAATA	CCCGATCCAG	gtaagttggg
6	148	tcgatttcag	ATGTTTATGG	ACCATTCACG	gtaagatgag
7	149	tcttttgcag	ACATAAGAAA	TGCCCCTGTG	gtaagagtta
8	108	cctccttcag	GCATTTAGTG	GAGAATGAAG	gtataagtaa
9	279	ttaatctcag	AAAATCCTCA	GGTGAGAAAG	gtgagtgtat
10	72	tctctgacag	GGGAAGGTCT	CCTAGGACAG	gtgagtgtgt
11	125	atcgctctag	ATGCAGTTAC	ACCACCAAAG	gtattattaa
12	73	atgtctacag	GTACCAACAC	CCTGACTGAG	gtaagcagag
13	204	ctgtccacag	ATTGGAGAGC	CCAGTTGCAG	gtgactggga
14	135	gtctctgcag	TTCCTGGAGT	GCAATTCAAG	gtaaactgca
15	76	ttatctccag	GATCCAGAGC	GAAGACGCTG	gtacagtcag
16	69	ctcatcctag	TCTTGGCTTC	GACACAAACG	gtatttacca
17	90	gtctctgcag	CTCCCGCTCA	GCTTCTGGAG	gtttagtata
18	104	tctccggcag	GGTACCTGGT	GGGTTCCCAG	gtgagtttcc
19	194	tgtgttgcag	GTCGTCTGTG	GAGTATTTAATA	caaggtagaa
20	229	ttctaccctc	AGATCGTCAG	TTCTTTTACG	gtaggattat
21	138	tcccccacag	CATCTTCCAT	GCATCAGCAA	gtgagtggat
22	187	ttgactttag	GTTTAAGACA	CATCATCCAG	gtaacggctg
23	90	ttcccaacag	CTCAGTGGAT	GTACATTTTG	gtaaggaatg
24	190	tgcttttcag	ACCTGTGTTC	ACGGGCTCCG	gtgaggacag
25	160	ttgtccccag	GAAAATCATC	GTACAGTAAG	gtagctgttt
26	79	ttcgttgcag	GTACAACTTG	GAGAGACACA	gtacgtcttg
27	114	tgttttatag	ATAATGAAAC	TAATTCAAAA	gtaaggaaac
28	165	tccttaacag	ATCATTCTCC	AAATGGGAAG	gtgcaggaaa
29	464	tgattttcag	GTGATTGAGT	CCTGGATTTT	gttaccagac

[a] The partial sequences of the introns proximal to the 5′- and 3′-ends of exon 3 are not available, therefore they are represented by 'nnnn'.